Final Report

Development of Liquid-Vapor Core Reactors with MHD Generator for Space Power and Propulsion Applications

DOE Project: DE-FG07-98ID 13635

Principal Investigator
Samim Anghaie
Department of Nuclear and Radiological Engineering,
University of Florida

August 13, 2002

TABLE OF CONTENTS

INTRODUCTION

Any reactor that utilizes fuel consisting of a fissile material in a gaseous state may be referred to as a gaseous core reactor (GCR). Studies on GCRs have primarily been limited to the conceptual phase, mostly due to budget cuts and program cancellations in the early 1970's. A few scientific experiments have been conducted on candidate concepts, primarily of static pressure fissile gas filling a cylindrical or spherical cavity surrounded by a moderating shell, such as beryllium, heavy water, or graphite. The main interest in this area of nuclear power generation is for space applications. The interest in space applications has developed due to the promise of significant enhancement in fuel utilization, safety, plant efficiency, special high-performance features, load-following capabilities, power conversion optimization, and other key aspects of nuclear power generation [1].

The design of a successful GCR adapted for use in space is complicated. The fissile material studied in the past has been in a fluorine compound, either a tetrafluoride or a hexafluoride. Both of these molecules have an impact on the structural material used in the making of a GCR. Uranium hexafluoride as a fuel allows for a lower operating temperature, but at temperatures greater than 900 K becomes essentially impossible to contain. This difficulty with the use of UF_6 has caused engineers and scientists to use uranium tetrafluoride, which is a more stable molecule but has the disadvantage of requiring significantly higher operating temperatures.

Gas core reactors have traditionally been studied in a steady state configuration. In this manner a fissile gas and working fluid are introduced into the core, called a cavity, that is surrounded by a reflector constructed of materials such as Be or BeO. These reactors have often been described as cavity reactors because the density of the fissile gas is low and criticality is achieved only by means of the reflector to reduce neutron leakage from the core. Still there are problems of containment since many of the proposed vessel materials such as W or Mo have high neutron cross sections making the design of a critical system difficult. There is also the possibility for a GCR to remain in a subcritical state, and by the use of a shockwave mechanism, increase the pressure and temperature inside the core to achieve criticality. This type of GCR is referred to as a shockwave-driven pulsed gas core reactor. These two basic designs were evaluated as advanced concepts for space power and propulsion.

STEADY STATE GAS CORE REACTORS

Solid core reactors provide the path of minimum risk for generating nuclear space power in the coming decade. These reactors can be expected to achieve evolutionary improvements in their performance based on modest extrapolations of current fuel technology. In contrast, liquid gas and vapor core reactors offer a path for extraordinary improvements in performance, and have the highest potential for reducing overall system specific mass [2, 3]. Some key features of gas core reactors include:

- In space assembly and fueling
- Safe fuel delivery and handling
- Power is generated at high temperatures and heat is rejected at high temperatures—high flexibility in minimizing the radiator size and weight
- Power scaling and choice of conversion technique are practically unlimited—power level and quality can be accommodated by adjusting fuel circulation rate and the average fuel exit temperature

- For surface power generation, a completely passive, gravity driven, ultrahigh burnup and very long life system is achievable
- Very low fuel development cost, testing, and facility requirement

Liquid and gaseous core reactors impose minimum geometrical constraints on the fuel configuration while providing a high temperature heat source plus a powerful ionization source. These features lead to the inherent technical advantages of energy conversion temperatures that are not limited by fuel integrity limits, and working fluid properties that are enhanced by the ionization processes. High conductivity of the fissioning plasma/working fluid allows for the use of magnetohydrodynamic (MHD) energy conversion in those systems (see Figure 1).

The steady state system illustrated in Figure 1 is for a 3 m^3 gas core reactor with MHD energy conversion with net cycle efficiency of 22%. Other analyzed system parameters include a neutron flux level of 10^{15} n/cm2 sec, nuclear enhanced electric conductivity of 60 mho/m, and a magnetic field of 4 Tesla.

These technical features lead to design advantages that include high working fluid and heat rejection temperatures, high fuel utilization (burnup up to 200,000 MWd/MT), elimination of fuel fabrication, testing, and verification, simplified fuel management, inherent hot spot compensation, and flat power density profiles [4, 5]. Another attractive liquid core reactor system is a uranium-droplet core nuclear rocket. Basic features of such system have been described in reference [6].

Operationally, these design advantages lead to mission benefits and improved safety. These include lower trip times and initial mass in orbit, reduced radiator mass, the potential for reactor refueling and reuse due to the fluid nature of the fuel, and a zero probability of accidental criticality on launch since the reactor is launched unfueled.

The primary focus of this research project was to establish the scientific and technical feasibility of ultracompact (mass to power ratio = 0.5 to 2.5 kg/kWe), tens of megawatt nuclear electric power systems that could be used for 100 to 200 day class piloted Mars mission or for interplanetary and interstellar missions. Gaseous core reactors fueled with liquid uranium droplets or uranium tetrafluoride are primary systems, which are considered for this analysis. Both disk and linear MHD generators are to be considered for conversion of the enthalpy of partially ionized fissioning plasma to electricity.

Gaseous and liquid droplet core reactors can potentially provide the highest reactor and cycle temperature among all existing or proposed fission reactor designs. This unique feature makes this reactor concept a very natural and attractive candidate for very high power (10 to 1000 MWe) and low specific mass (0.5 to 2.5 kg/kWe) nuclear electric propulsion applications. The fuel temperature is the main limiting factor in operation of solid fuel reactor cores. Compact size and low mass requirements for space reactors with solid fuel structure demand very high heat transfer at the fuel-coolant interface. The low thermal conductivity of ceramic fuel materials results in very steep temperature gradients, which in turn yield undesirable high fuel and low coolant temperatures. The fuel-coolant interfacial heat transfer is no longer a limiting factor for operation of gaseous core reactors. Furthermore, the low thermal conductance of gaseous fuel allows very high average bulk fluid temperature while maintaining wall temperatures significantly cooler.

Critical Issues For Vapor Core Reactor Development For Power And Propulsion

Modeling of the vapor core reactor (VCR) includes coupling with either a disk or line magnetohydrodynamic (MHD) power conversion system. The reactor and MHD generator are illustrated in Figure 2 below with a central gas core surrounded by a reflector/moderator of beryllium oxide (BeO). This region of BeO is what provides the slowing down (moderation) of fission neutrons to allow for thermal fissioning of U-235 in the core.

This analysis is based on a typical VCR-MHD system, 200 MWe power could be generated in a disk MHD that is fed by more than 1100 MW thermal power in a 3-m^3 reactor core with a 50 cm BeO reflector region. The VCR operates with uranium tetraflouride (UF_4) as the fissioning fuel. Analysis was done with potassium fluoride (KF) as the working fluid with other candidate working fluids including K, Li, Na, KF, LiF, NaF, etc. The fuel UF_4 is vaporized in the reflector/moderator region prior to injection into the core. The KF working fluid provides cooling for an inner containment vessel prior to entering the core. Fissioning of the fuel in the core region is used to heat the UF_4/KF mixture to 4000 K at the reactor exit.

Reactor

Some critical issues associated with the fissioning plasma core were identified in this study. The fissile content and neutronic compatibility of fluids and structural materials must be matched to the optimal power density and desired temperature profiles. In particular, detailed neutronic analysis is required for the effects of the pressure vessel and necessary structural and piping materials shows that the required fissile gas density is much higher (>20 MPa) as shown in Figure 3 than the approximately 2 MPa that would be required for a 3 m3 core with only a BeO reflector. Therefore, for reasons of neutron economy, tungsten and tungsten alloys cannot be used. Instead, materials such as the alloy TZM (Mo99, Ti0.9, Zr0.1) are necessitated both from a materials and a neutronics perspective. Concomitantly, power density and temperatures are limited by capability to cool the walls (heat flux limited, not temperature limited). Tangential injection cooling along the length of the pressure vessel will be required. In addition to the above constraints, issues of material compatibility must be addressed since the chemistry of fluids impacts on entire system design. Table I summarizes the compatibility of six high temperature materials with both UF_4 liquid and vapor. However, as mentioned above, materials such as W or Mo could only be used on a limited basis due to their high neutron cross sections.

Table I. Survey of material compatibility with UF_4 liquid and vapor based on test data or chemical thermodynamic analysis.

Materials	**UF_4 Liquid (1300 < T < 1700 K)**	**UF_4 Vapor (1700 < T < 3000K)**
C	Fully Compatible	Fully Compatible T<3000K
W	Fully Compatible	Fully Compatible T<3000K
Re	Fully Compatible	Fully Compatible T<2600K
Mo	Fully Compatible	Fully Compatible T<2000K
WC	No Reaction	No data
Mo_2C	No Reaction	No data

A comparison of the UF_4 and U metal saturation vapor curves is shown in Figure 4. At the l0-20 atmospheres of core pressure required for criticality, U metal boils at around 5000K, a temperature significantly beyond material limitations at different regions in the power cycle. Considering the vapor or liquid recirculation of U metal, criticality, condensation and vaporization problems, UF_4, appears to be a more suitable fluid for vapor core systems. However, the use of UF_4 requires additional research on the chemical, materials, thermodynamic and electrical conductivity issues critical to "magnetic turbine" energy conversion. Also, uranium metal, in liquid form, as micron size droplets dispersed in a vapor working fluid in microgravity, could offer significant potential for further performance gains, especially if the droplets can be separated from the working fluid as it exits the core. Other gas core concepts have examined the use of UF_6 as the nuclear fuel. However, as shown in Figure 5, UF_6 is chemically unstable, while UF_4 is stable. This stability is also born out in Figure 6 illustrating the high bond dissociation energy of UF_4 in comparison with other uranium halides.

For UF_4 Rankine cycle, the fuel should be vaporized before injection to the core. In the present model, energy generated by fissions occurring in the fuel stream piped through the reflector/moderator prior to entry to the core is assumed as the heat source for vaporization of the fuel. This is a very complex phenomenon requiring a detailed study involving coupled neutronic, computational fluid dynamics, and heat transfer analyses. Because the present model calls for highly enriched uranium, a minimum recirculation of fissile material is required for low fissile inventory and criticality control.

MHD Nozzle and MHD Duct

Figure 7 and 8 concisely illustrates the geometry and electrodynamics of a Hall type MHD generator respectively. Two of the dominant critical issues in a system using UF_4 or uranium and metal fluoride working fluid are attainment of electrical conductivity and the velocity of the mixture within the MHD channel. The electrical conductivity of the plasma in the MHD channel is determined primarily by the conditions established in the fissioning gas core and the subsequent processes occurring in the generator channel. Large uncertainties in the knowledge base of collision cross sections and kinetic properties of the plasmas expected in these systems makes the calculation of electrical conductivity difficult and the accuracy of the results uncertain. The changes in chemical composition of the uranium compound and working fluid mixture due to high temperature and irradiation significantly impacts both the conductivity and the velocity within the channel. Furthermore, multiple mechanisms contribute to the attainment of conductivity -- equilibrium ionization with the addition of (possibly seed material), electric field non-equilibrium heating, and ionization from fission fragments and the radiation field in the channel.

For a given channel ratio, conductivity does not affect efficiency directly (only through losses) but governs channel length as seen in Figure 9 for the effect of both conductivity and magnetic field strength. So if either conductivity or magnetic field strength or both can be increased, then a more compact and lighter weight design might be possible. This assumes that the steps taken to achieve these improvements do not negatively impact on the size or specific mass of the system.

The nozzle and duct are the most vulnerable components from a materials standpoint for fluid temperature energy conversion (very high heat transfer, erosion, etc.). These components require major cooling systems and high temperature materials. An upper limit to nozzle and duct

temperature is set at 2500 K. Magnets also could have significant cooling requirements when placed close to the core to enhance channel ionization.

Analysis indicates both disk and line MHD generator with segmented electrode could be used. Buildup of conductive deposits between the electrode segments that may provide a short circuit path between segments is another potential problem. This is a critical issue that needs to be addressed in future phases of the MHD duct design. One of the principle impediments to the design of disk MHD generators is the need to have a high swirl number. Because of the high gas temperatures, encountered in the VCR the addition of any mechanisms to enhance swirl would be problematic.

Conversion efficiency is a function of Mach number, electrical loading parameter and ratio of specific heats (as γ/γ-1). For enthalpy extraction ~25% at a channel ratio in the range of 30 to 40, the specific heat ratio has to be >1.15 (due to γ/γ-1). Vapor expansion criteria are dominant.

Condensing Radiator

A compact and light space radiator for plant heat rejection is an enabling component for multi-megawatt power generation. The issues of reliability and survivability escalate with radiator size. Besides the many possible radiator shapes and physical arrangement variations, the absolute measure of the heat rejection effectiveness is the T^4 dependence. Shown in Figure 10 is a graph depicting the radiator mass-to-power ratio as a function of radiator inlet temperature. Shown on this graph are data points for different systems. The abscissa is marked with potential candidate working fluid boiling temperatures. A UF_4-fueled vapor core, operating in a closed Rankine cycle (essentially constant radiator temperature), improvement clearly offers the capability of order-of-magnitude in radiator performance.

Advanced, high temperature and lightweight materials such as SiC reinforced Ti with carbon/graphite composites for the fins could prove useful in the design lightweight radiators (~6 kg/m^2) for a lower system specific mass [7]. Two-phase flow of a fuel/working fluid mixture in microgravity in general requires experimental definition. In the absence of gravity, cyclone separators might be considered to separate the liquid phase from the gas. This is an area that requires additional research.

MPD Thruster

An ultra-high power nuclear electric propulsion system requires simultaneous optimization of the thruster and power generation system. The MHD output power should be conditioned to directly feed the thruster current and voltage needs. Both MHD channels and Magnetoplasmadynamic (MPD) thrusters tend to produce and consume high currents at relatively low voltages. This could potentially eliminate or at least, dramatically reduce the power management and conditioning needs in these systems. The high breakdown voltages that are needed to establish the arcs in MPD could be generated with a compact power storage system. The direct coupling of MHD output power to generate plasmoid pulses in MPD could produce a few grams to multiple kilograms of thrust at very high specific impulse (I_{sp} = 1500 to 10,000 s.) In essence, the coupled MHD-MPD propulsion system operates like a transformer; converting the energy of very high mass flow rate and relatively low velocity of the VCR plasma to very low flow rate and extremely high velocity of the thruster plasma. The order of magnitude reduction in specific mass and very high specific impulse of VCR-MHD/MPD system could lead to dramatic reduction in the cost of interplanetary as well as interstellar missions.

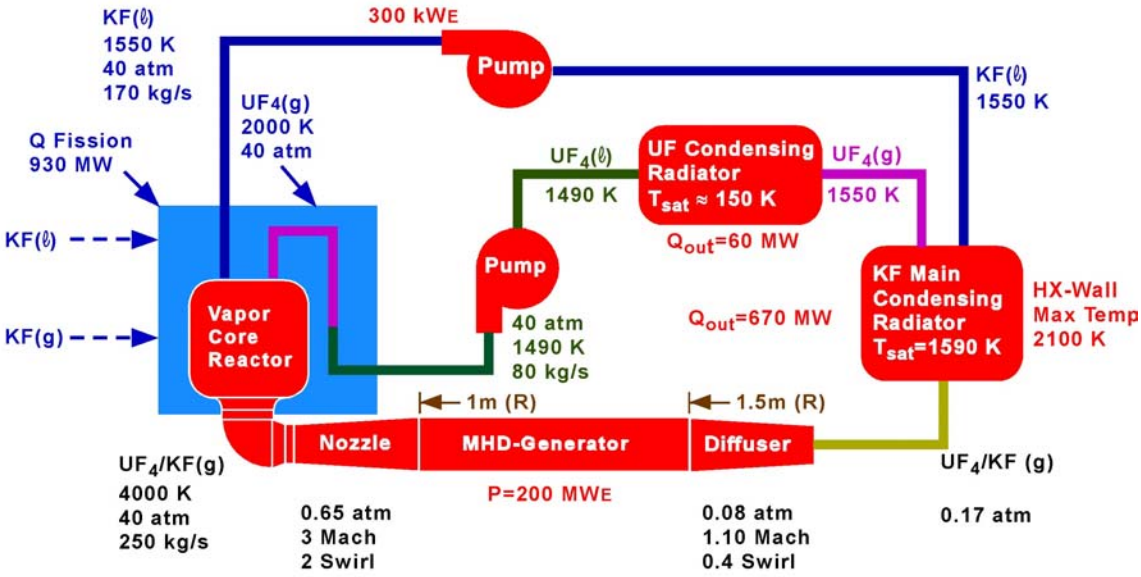

Figure 1. Illustration of a 200 MWe gas core reactor with MHD energy conversion in a closed Rankine cycle (specific mass 0.37 kg/kWe.)

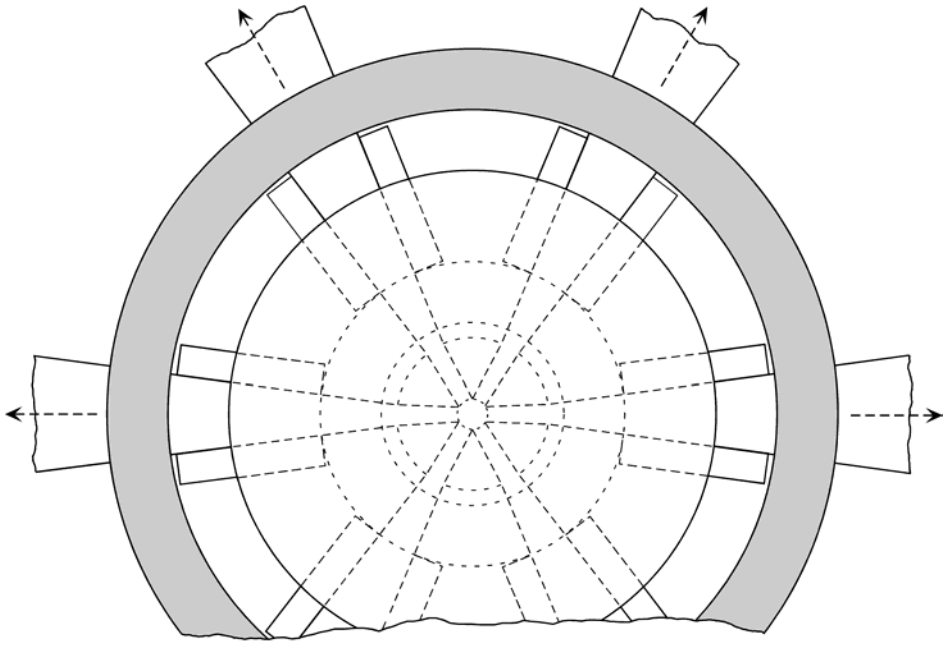

PARTIAL TOP VIEW

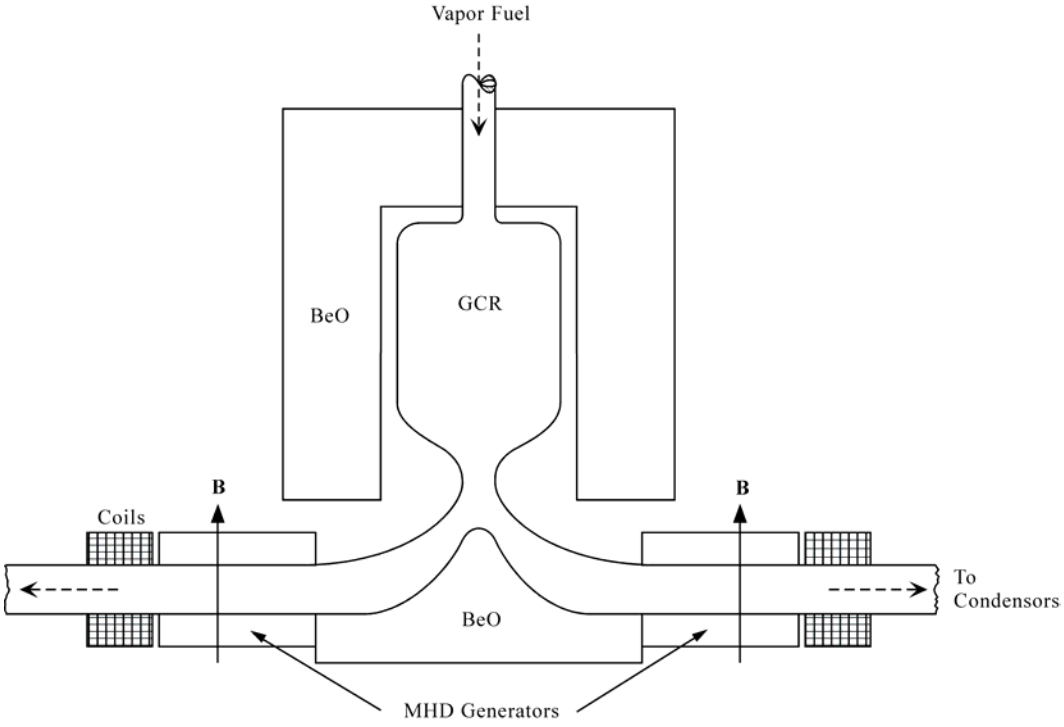

FRONT VIEW

Figure 2. Schematic illustrations of the fissioning plasma core reactor and line MHD generator.

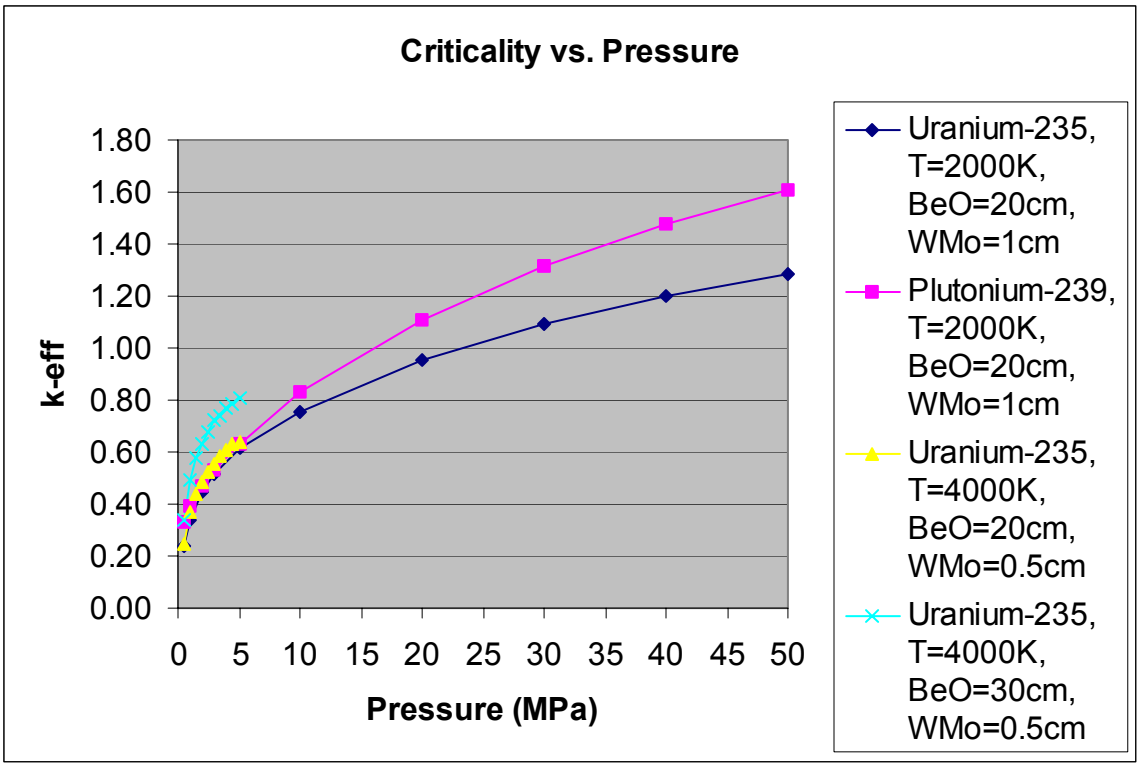

Figure 3. K-effective calculated for different core/reflector/vessel designs with U-235 or Pu-239 as the fissile gas, BeO as the reflector material, and various thicknesses of W/Mo as the core vessel.

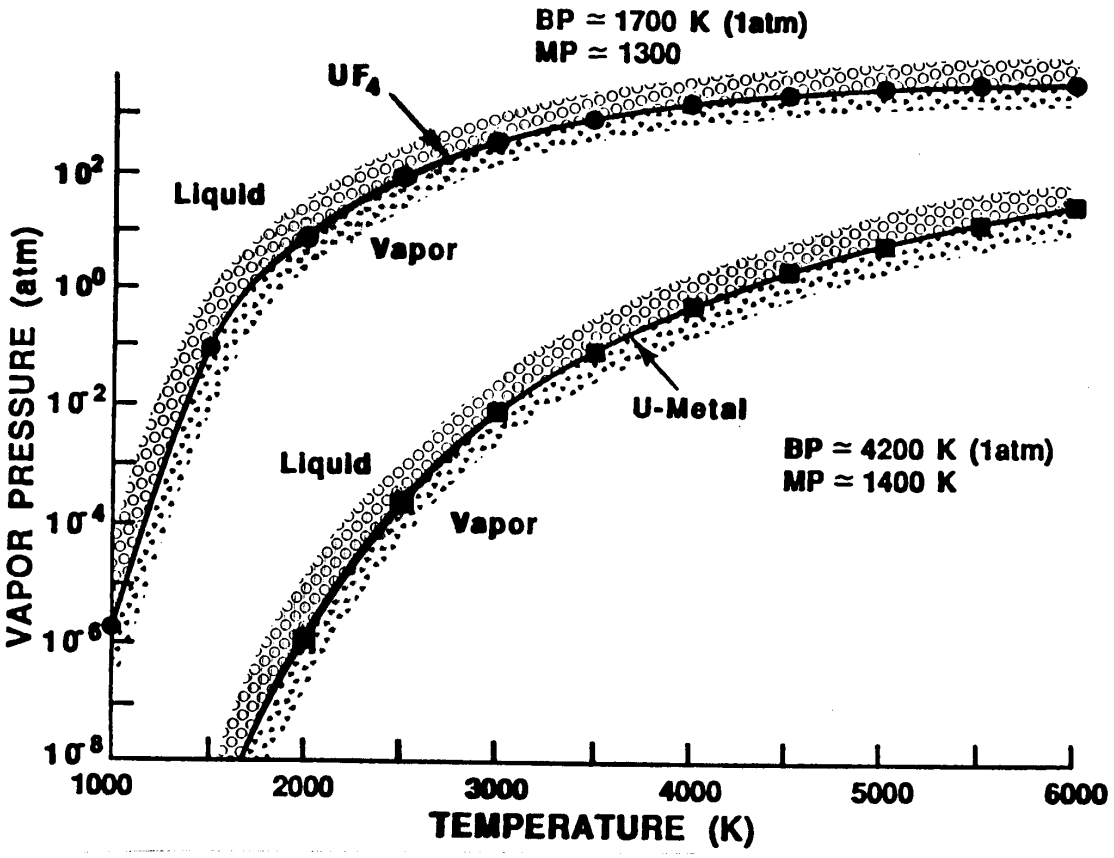

Figure 4. Vapor pressure of UF_4 and uranium metal as a function of temperature.

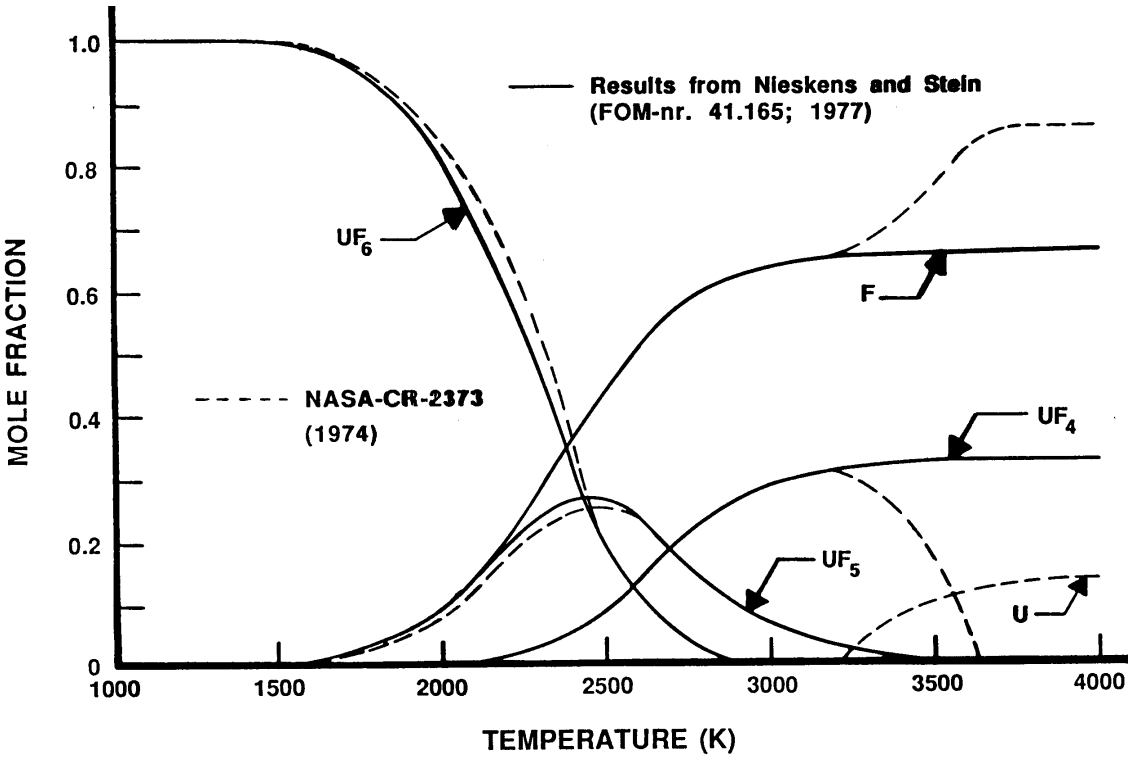

Figure 5. Mole fraction of constituent species of uranium-fluorine system versus temperature at 1 atmosphere.

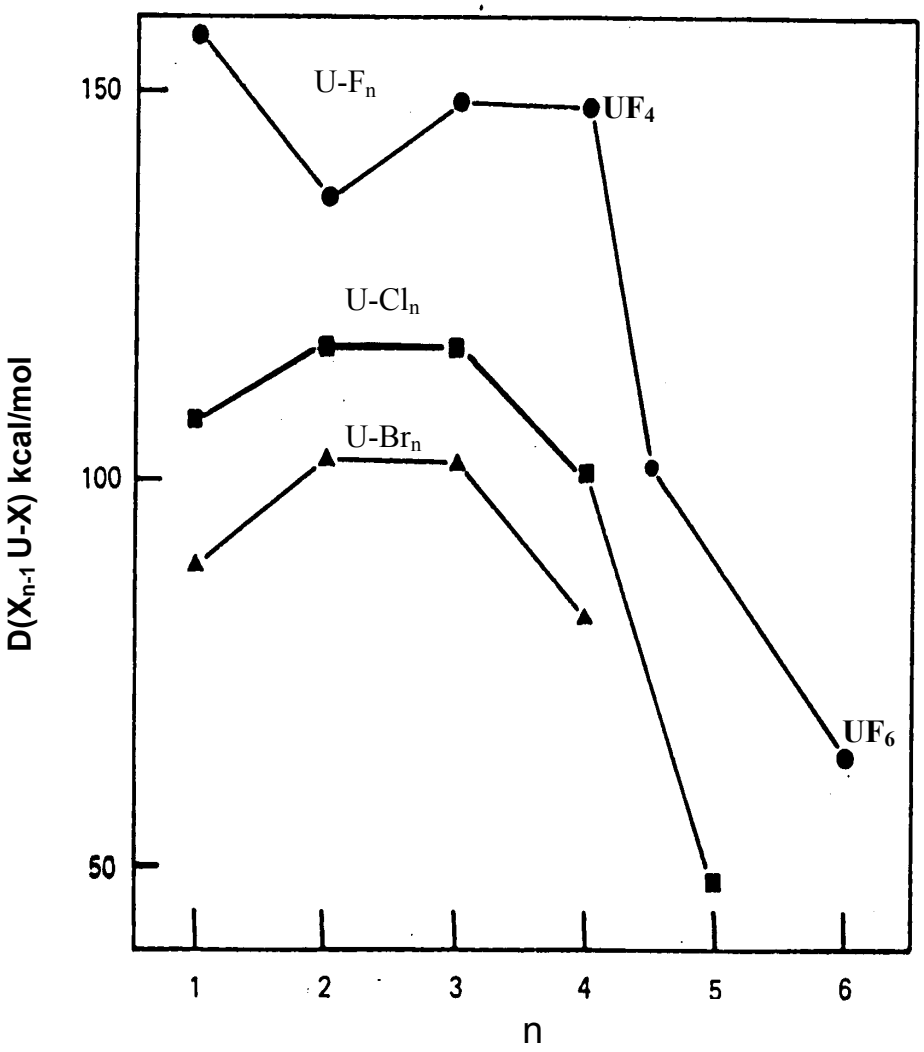

Figure 6. Trends in individual bond dissociation energies for the uranium halides

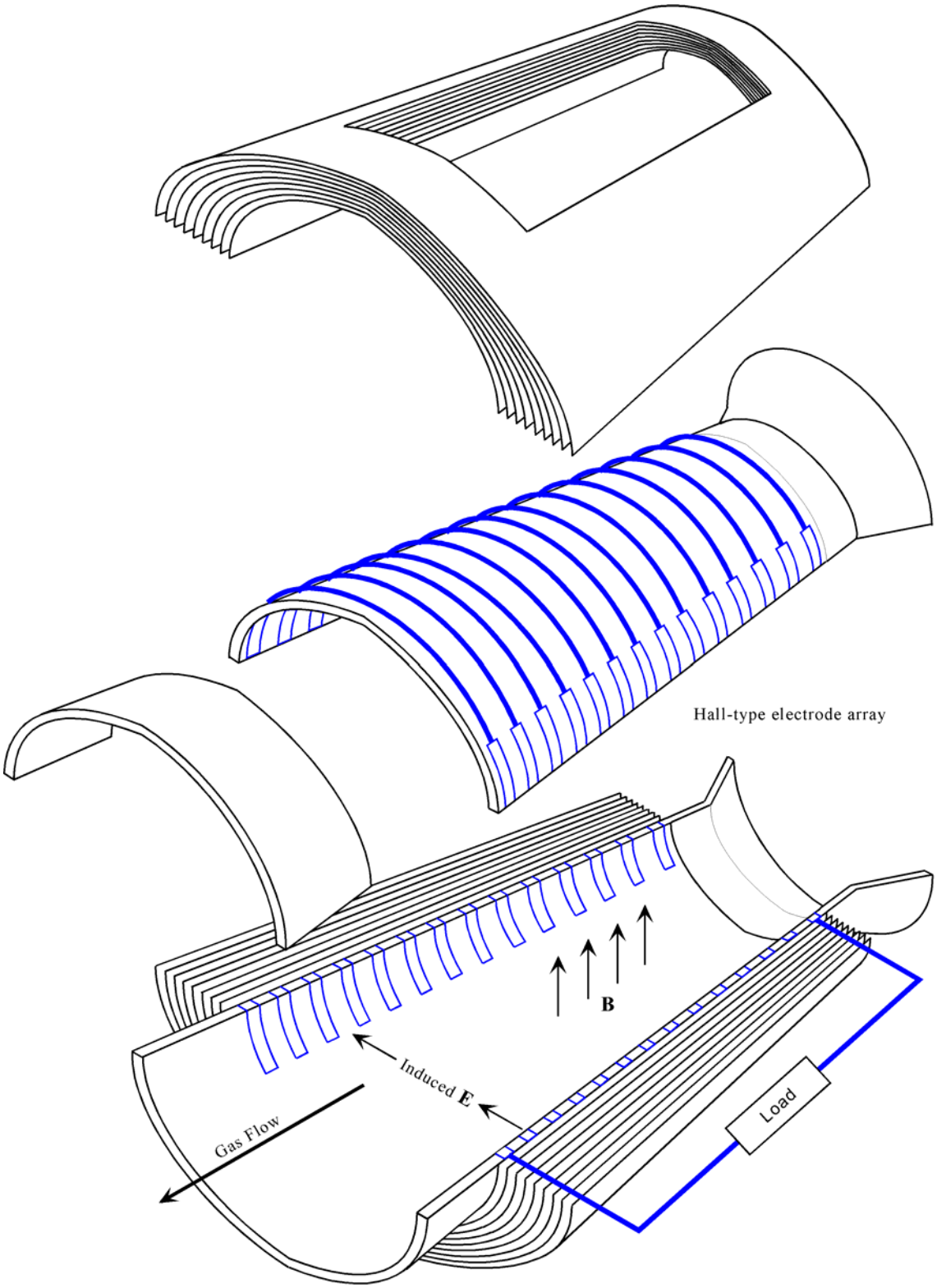

Figure 7. Exploded view of a Hall type MHD generator

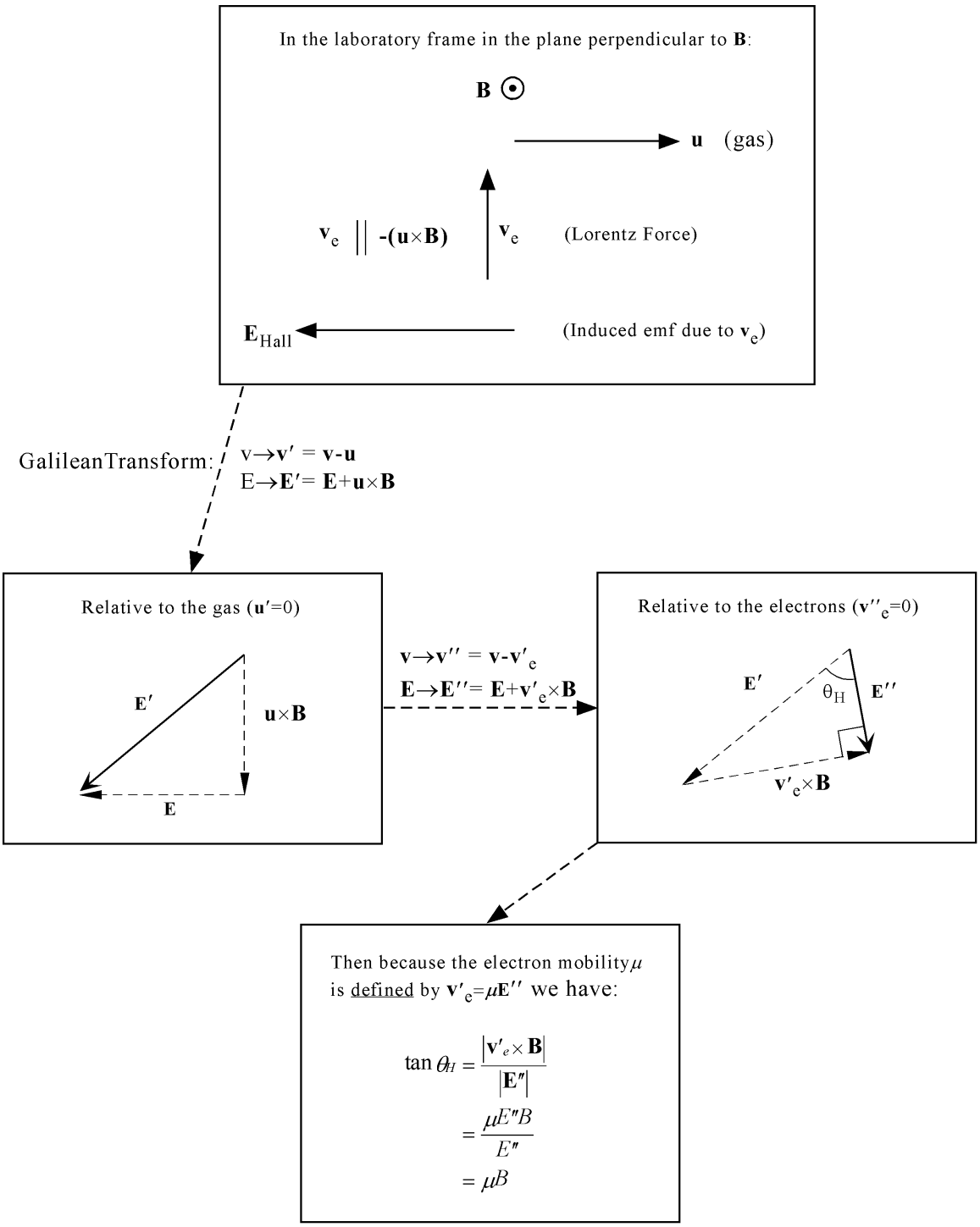

Figure 8. Electrodynamics of a Hall MHD generator.

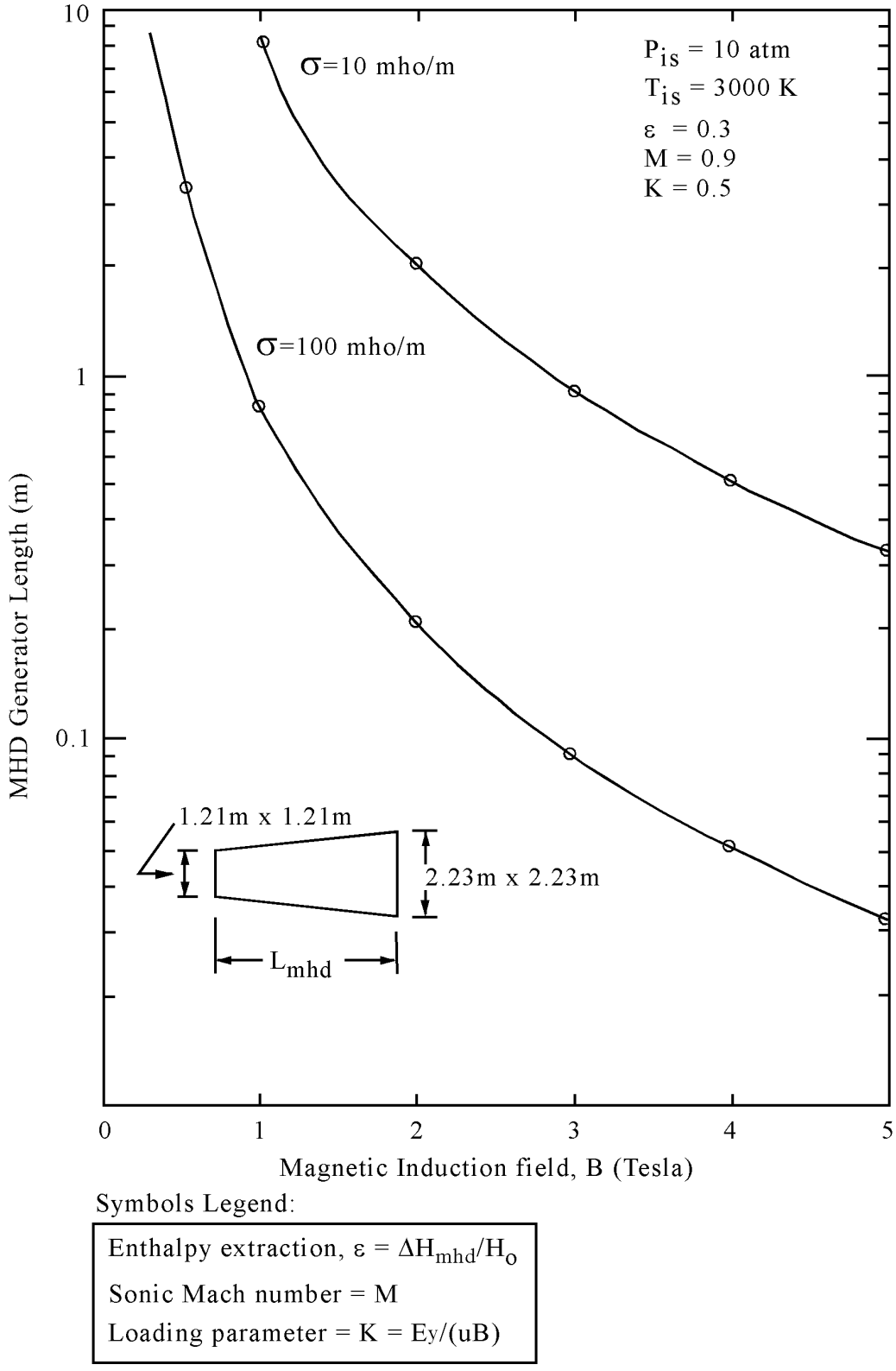

Figure 9. Effect of conductivity and magnetic field on MHD generator length.

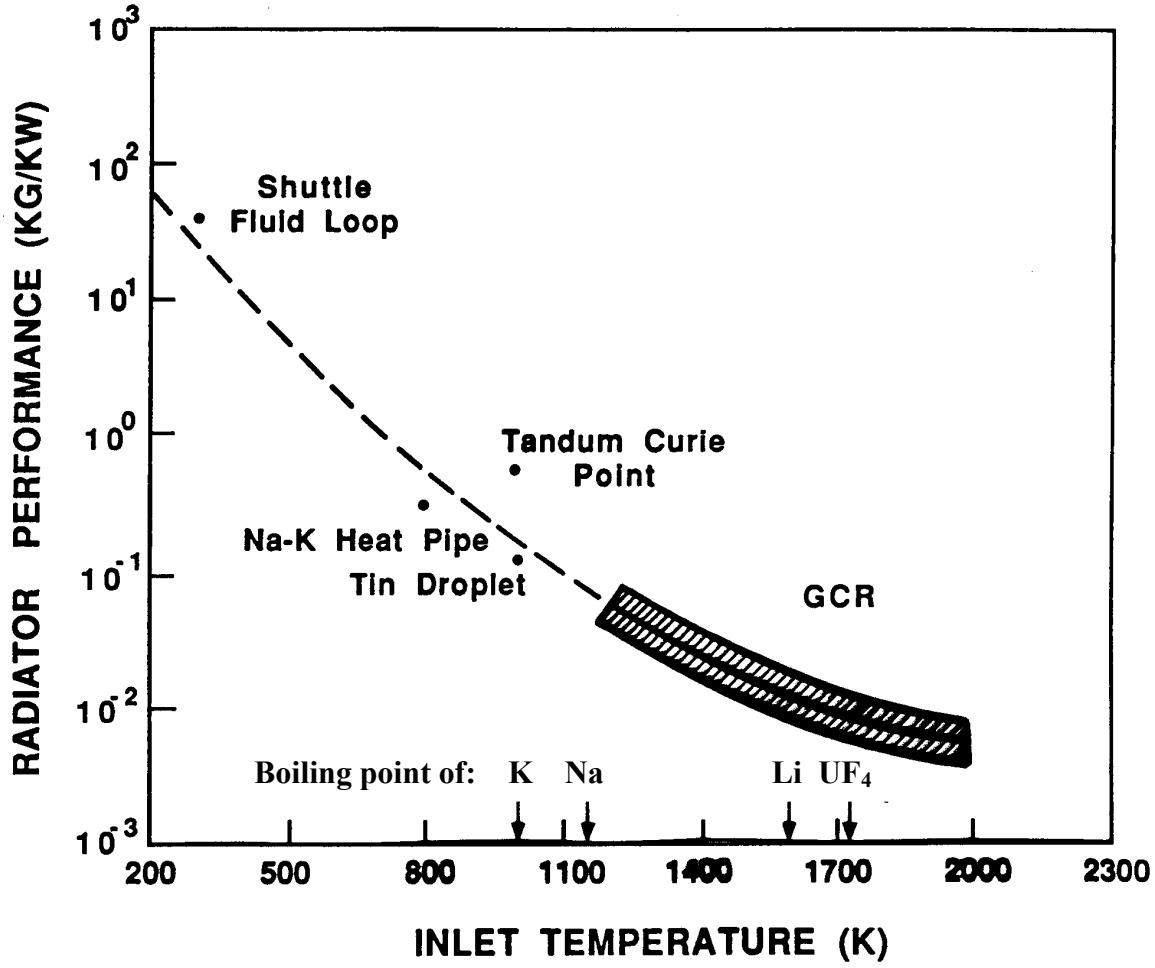

Figure 10. Radiator mass to power ratio as a function of temperature.

PULSED GAS CORE REACTORS

A pulsed, or burst, gas core reactor can operate in several different ways, but the premise, regardless of the method of operation, is still the same. When power is not needed the core remains at a subcritical fuel density. Then when power is needed a driving mechanism causes the fuel density to increase dramatically. Criticality can be achieved by either decreasing the physical volume of the core, as with a piston driven pulsed gas core reactor [8], or decreasing the active volume of the core, as with a pulsed magneto-induction gas core reactor (PMI-GCR). A piston driven reactor requires moving parts and may not be the best design for space applications due the inherent difficulty of maintaining a mechanical system in a micro or zero gravity environment. A PMI-GCR, which uses large magnets at opposite ends of a cylindrical core to generate opposing pulses that combine together in the center to achieve criticality, may prove to be an ideal design for interplanetary environments [9].

Shockwave Mechanics

In the case of two colliding shockwaves, one can consider a single shockwave traveling towards a solid, rigid wall and its reflection from that wall. Because of the symmetry of the pulsed gas core reactor it can be reasoned that such a model is accurate due to the conservation of energy and momentum. Using fluid-gas dynamics and thermodynamics, one can obtain the excess pressure ratio at the point of reflection:

$$\frac{p_2}{p_1} = \frac{\left(2\mu^2 + 1\right)p_1 \big/ p_0 - \mu^2}{\mu^2 \, p_1 \big/ p_0 + 1};$$

$$\mu^2 \equiv \frac{\gamma - 1}{\gamma + 1};$$

$$\gamma = \frac{C_p}{C_v}$$

where p_0 is the initial fissile gas pressure, p_1 is the shock front gas pressure, and p_2 is the pressure at the point of interaction.[9] γ is the ratio of the heat capacity at constant pressure and the heat capacity at constant volume. The value of γ is known for most gases from experiment, and for uranium tetrafluoride is approximately 1.06. For strong normal shocks where p_1/p_0 is much greater than one, the excess pressure ratio reduces to:

$$\frac{p_2}{p_1} \approx 2 + \frac{\gamma + 1}{\gamma - 1};$$

Inserting the value for γ reveals that the shockwave pressure after the interaction can be as high as thirty-six times greater than the shockwave pressure before the interaction.[9] Figure 11 demonstrates the phases of an interaction between to opposing shockwaves.

Project Objectives

The main constraint on this pulsed gas core reactor is that it remains subcritical, with an approximate neutron multiplication factor, k_{eff}, of 0.99, when the core is offline. Using MCNP 4C,

a Monte Carlo simulation code, core dimensions were analyzed to minimize leakage. Because of the unique nature of a PMI-GCR it may operate as either a fast or thermal reactor so both possibilities must be studied, with appropriate materials for the reflector in order to take advantage of either case. The overall purpose of this phase of the project was to determine if a PMI-GCR can achieve criticality, and to minimize the weight of the system since it is primarily being adapted for space applications

Modeling a PMI-GCR

MCNP 4C was used to determine the feasibility of a PMI-GCR achieving criticality. When modeling a PMI-GCR there are high levels of uncertainty due to the supersonic shockwaves driving the fission process. Shockwaves will ionize and heat up the fuel as they travel through the core, which will reduce the need for constant extreme heating used in static pressure GCRs. Actual operating temperatures cannot be known until more detailed fluid dynamic modeling is done. However, by using several assumptions, more realistic data can be extrapolated from the results gathered during this project.

A cylindrical cavity with a reflector surrounding the lateral surface was used in determining the criticality of a PMI-GCR. The cavity is filled with 100% enriched uranium-235 metal at gas densities, which is derived from the ideal gas law and is expressed as the product of the pressure of the fissile gas and the molar weight of uranium-235 divided by the product of the gas constant and the system temperature (Eq. 1). The temperature of the reflector and the gas were kept at 300 K because actual operating temperatures for a PMI-GCR are not implicitly known. The information gathered at a gas temperature of 300 K can be used to extrapolate values at actual operating temperatures.

$$\rho = \frac{PA}{RT} \qquad \text{Eq. 1}$$

Modeling a cylindrical core in MCNP is not difficult and important criticality information can be gathered from the model. The MCNP code is used to simulate particle transport. Unlike deterministic methods, Monte Carlo does not try to solve an explicit equation, such as the Boltzman transport equation, but rather obtains values by simulating actual behavior of individual particles and recording some aspects of their behavior. The behavior of each particle is determined by the probability of a type of interaction occurring in the medium. By using tally cards in the input file the behavior of the neutrons can be easily sorted and analyzed.

For this project, a cylinder was set up along the x-axis, centered on the origin (Figure 12). The starting fission source was placed at the origin and the neutrons generated were tracked as they travel through the core and reflector, until they leave the system or are eliminated by an interaction. Using tallies information will be gathered pertaining to axial flux and leakage from the system. In order to limit excess computational time neutrons with energies lower than 1.0^{-10} MeV or higher than 15.0 MeV will be removed from the system.

Reactor Leakage

The general design of GCRs involves a cylindrical cavity containing a fissile material in a gaseous compound, such as $^{235}UF_4$, surrounded by a moderating reflector. The major difference between a conventional gas core reactor and a PMI-GCR is that the top and bottom parts of the cylinder will need to be open for the placement of the mechanisms that drive the shockwaves. The lack of a reflector at the top and bottom of the cylinder requires that moderation be performed by the

reflecting material surrounding the lateral wall of the core. A quantity referred to as reactivity will be used to study the gains achieved in system criticality by increasing specific variables, such as gas pressure or reflector thickness. Reactivity, ρ, is defined as the fractional step change in the effective neutron multiplication factor between two states of the core (Eq. 2). [10]

$$\rho = \frac{k_2 - k_1}{(k_1 + k_2)/2} \qquad \text{Eq. 2}$$

The first goal of this study was to find a reactor size that minimizes leakage from the core. Keeping the same core volume, the ratio between the cylinder's height and diameter will be increased from 1.0 to 3.0 in increments of 0.25. Each system will have a beryllium oxide, BeO, reflector 20 cm thick, with gas pressures of 5, 10, 15, and 20 atm at 300 K (Table 2). Table 3 shows the cylinder dimensions used for a constant volume of 30 m^3. The normalized total leakage for each system will then be plotted as leakage versus pressure on a single graph and any differences between the k_{eff} at various height-to-diameter ratios will be evaluated. There will be a point where increasing the height-to-diameter ratio will yield less leakage loss than the previous point. That design was then used in the following sections.

Gas Pressure (atm)	Density (g/cc)
5	4.77E-02
10	9.55E-02
15	1.43E-01
20	1.91E-01

Table 2. Gas densities for uranium-235 gas at 5, 10, 15, and 20 atm at 300 K.

Ratio	Height (cm)	Radius (cm)	Surface Area (m^2)
1.00	336.8	168.4	53.4
1.25	390.8	156.3	53.7
1.50	441.3	147.1	54.4
1.75	489.1	139.7	55.2
2.00	534.6	133.7	56.1
2.25	578.3	128.5	57.1
2.50	620.4	124.1	58.0
2.75	661.0	120.2	59.0
3.00	700.5	116.8	60.0

Table 3. Height and radius, in cm, of the cylindrical core used in the MCNP input for varying height-to-diameter ratios, but a constant core volume of 30 m^3. The BeO reflector is an annular cylinder with a radius 20 cm greater than the core.

Reflector Material and Thickness

Uranium-235 has a large fission cross section for neutrons at energies below 1.86 eV, also known as thermal neutrons. Most commercial power reactors in the world use light water, H_2O, to moderate neutrons to thermal energies. For space applications the use of water is an impossibility so another material is needed. A candidate material is beryllium, in the form of beryllium oxide (BeO). BeO, with a density of 3.7 g/cc, is a white ceramic material often used for special nuclear reactor applications. It will be used as the moderating reflector for the thermal reactor model. Tungsten-184 will be used as a reflector on the fast reactor model because it should not moderate the neutrons but reflect enough of them back into the core to sustain a fission reaction. Tungsten has the benefits of a very high density, 19.2 g/cc, a melting point of almost 3700 K, and the isotope ^{184}W has a very low absorption cross section.

The purpose of this part of the project was to determine at what thickness do the materials become saturated, or no longer yield significant gains in reactivity. Tungsten thickness will range from 1 to 20 cm and BeO thickness will range from 10 to 40 cm. Once the optimum thickness for the fast and thermal models have been determined, the gas pressure inside the core will be analyzed to find the requisite subcritical state with a k_{eff} of approximately 0.99. Fast reactors using solid fuel require 4 to 5 times the amount of fuel that a similar power rated thermal reactor uses. It is expected that the thermal PMI-GCR model will achieve criticality between 5 and 15 atm at 300 K, so the fast PMI-GCR model will be analyzed with gas pressures between 20 and 75 atm at 300 K.

Additional information was gathered in this section using the tally cards that may provide insight into the design of a PMI-GCR. Beryllium has a non-negligible (n, 2n) cross section and it is important to know how many of the neutrons per cycle are generated by this process. The mean neutron lifetime will be studied as well because as further details are gathered about the mechanics of the shockwaves driving the fission reaction the speed at which the neutrons travel to the reflector and back will become important. For a PMI-GCR to work as either a fast or thermal reactor the neutrons must be able to travel from the gaseous core, to the reflector, and back either before the original pulse that generated the neutrons has dissipated or in time to meet a following pulse. The pulse mechanism is part of the complexity in the design of a PMI-GCR. Although this particular area in the design of a PMI-GCR will not be addressed here the data will be collected to help future studies. Finally, the energy distribution of the axial neutron flux will be recorded with the aid of an energy bin card. An energy bin card allows the MCNP user to split up the flux output so that details about specific energy regions can be seen.

Approximations for various reactor types have been used in the past to help isolate neutrons of particular interest. This selection of an energy bin, or range, is done by comparing cross sections from various materials in the reactor. Using data collected individually by various laboratories around the world, nuclear reaction cross section information is gathered together to form the Evaluated Nuclear Data Files, also known as ENDF. The appropriate bins for the thermal and fast PMI-GCR models can be obtained by comparing the fission cross section for uranium-235 (Figure 13) with the total cross sections for tungsten-184 (Figure 14) and beryllium-9 (Figure 15). The bins are split up to isolate scattering resonances of the reflectors and the fission resonances of uranium-235 (Table 4 and Table 5).

Following the analysis of BeO and tungsten, other reflector materials will be studied to find comparative neutron multiplication factors and mean neutron lifetimes. The first to be studied will be hydrogen, in the form of zirconium hydride (ZrH_2) with a density of 6.5 g/cc. Hydrogen allows

for the greatest amount of energy to be transferred from a neutron during a collision because of its single proton nucleus. The next moderator studied will be deuterium, or heavy hydrogen, in the form of zirconium deuteride (ZrD_2), which also has a density of 6.5 g/cc. Although the amount of energy lost by the neutron during an inelastic scatter interaction is less due to deuterium's larger nucleus it is a far more stable atom and is essentially transparent to neutron absorption. Finally, high density graphite (ρ = 2.5 g/cc) will be analyzed. Graphite is used in some special reactor designs and will be good for comparing to BeO and tungsten.

Energy Bin	Lower Limit (MeV)	Upper Limit (MeV)
1	1.00E-10	1.00E-07
2	1.00E-07	1.00E-02
3	1.00E-02	4.00E-01
4	4.00E-01	1.50E+01

Table 4. 4-bin energy group used for the thermal PMI-GCR model.

Energy Bin	Lower Limit (MeV)	Upper Limit (MeV)
1	1.00E-10	1.05E-06
2	1.05E-06	4.00E-03
3	4.00E-03	1.50E+01

Table 5. 3-bin energy group used for the fast PMI-GCR model.

Simulating a Shockwave

After the core dimensions and subcritical fuel densities have been determined for both models a simulated shockwave interaction will be analyzed. The fuel mass will remain constant but the density will vary throughout the core (Figure 16). The center of the core will have a maximum pressure, P_H, of 100 atm at 300 K with a varying thickness, Δx. The remainder of the gas will be will be distributed evenly throughout the rest of the core with the pressure P_L. This does not accurately represent what occurs inside a core when two pulses moving at supersonic speeds interact, but should give some insight as to whether the cores can achieve criticality given a subcritical quasi-static state.

Reactivity Insertion due to Increasing Pressure

As a change in the pressure of the fuel occurs, the effective multiplication factor (or reactivity) will also change. This transient nature of the pressure inside a PMI-GCR gives rise to the need for a pressure coefficient of reactivity, represented as α_P, and has units of $\Delta k/k$ per atmosphere of pressure. This value allows for a quick evaluation of what will happen to k_{eff} if you reduce or increase the pressure in the core. One would simply multiply the change in pressure expected by the coefficient and that would give the resultant change in k_{eff}. Table 6 shows the gas densities that

correspond to pressures from 10 to 200 atm at 300 K, in increments of 10 atm, that will be used to calculate α_P for the fast and thermal PMI-GCR models.

Pressure (atm)	ρ (g/cc)	Pressure (atm)	ρ (g/cc)
10	9.55E-02	110	1.05E+00
20	1.91E-01	120	1.15E+00
30	2.86E-01	130	1.24E+00
40	3.82E-01	140	1.34E+00
50	4.77E-01	150	1.43E+00
60	5.73E-01	160	1.53E+00
70	6.68E-01	170	1.62E+00
80	7.64E-01	180	1.72E+00
90	8.59E-01	190	1.81E+00
100	9.55E-01	200	1.91E+00

Table 6. Density of uranium-235 gas from 10 to 200 atm at 300 K.

Reactor Leakage

Only the thermal PMI-GCR model was studied for this section because although the numbers would be different for the fast PMI-GCR model, the relationship between which dimension yields an adequate reduction in leakage should still be the same. Figure 17 shows the percent of source neutrons, or neutrons generated by fission, lost from the reactor versus the height-to-diameter ratio of the core for 5, 10, 15, and 20 atm gas at 300 K. Since a system with a great amount of leakage is more difficult to make critical than one with less leakage an evaluation of the neutron multiplication factor will aid in the selection of the best dimensions for the PMI-GCR.

Figure 18 is a plot of the k_{eff} versus the height-to-diameter ratio of the core for 5, 10, 15, and 20 atm gas at 300 K. Taking this information and plotting the ratio coefficient of reactivity versus the height-to-diameter ratio (Figure 19) indicates that a height-to-diameter ratio of 2.75 is the best choice. This ratio was chosen because the increase in reactivity for all for gas pressures begin to converge around this point. Also, interest in this reactor has been focused on a design with a cylindrical core with a length of 5 m and a diameter of 2 m. With a ratio of 2.75, a core 5 m in length would have a diameter of 1.82 m, which will be the dimensions used in the following sections.

Beryllium Oxide Reflector

Using BeO, the PMI-GCR can achieve the desired subcritical states at low pressures with an appropriate thickness. As the pressure of the uranium-235 gas increases the k_{eff} increases. Also, as the thickness of the reflector increases so does the value of the neutron multiplication factor. By analyzing the k_{eff} versus BeO thickness (Figure 20) a value of 30 cm at 10 atm yields a subcritical state with a k_{eff} of approximately 0.99. Although thinner reflectors at higher gas pressures also obtains the preferred subcritical k_{eff}, a thicker reflector allows for greater neutron scattering which improves the thermal spectrum of the neutron flux. Also, as shown in Figure 21, a thickness greater than 30 cm yields less of an increase in the effective neutron multiplication.

The mean neutron lifetime is given by MCNP in the units of "shakes", which is equal to 10^{-8} seconds. Figure 22 shows the mean neutron lifetime for the neutrons, which includes an action which terminates a tracked particle, such as an absorption or leakage from the system. The mean neutron lifetime is on the order of a few tenths of a millisecond and increases roughly linearly as the BeO thickness increases. Figure 23 shows the break down of the normalized axial flux for a core with a 30 cm thick BeO reflector and a pressure of 10 atm at 300 K. Leakage is primarily due to groups 3 and 4, as can be seen with the sharp decrease in the neutron population percentage towards the caps of the core. This is to be expected as neutrons in bins 3 and 4 have higher energies than bins 1 and 2. Also, the (n, 2n) reaction in beryllium-9 is found to be significant with 10 to 12 percent of the neutrons generated coming from this interaction. For the thermal PMI-GCR model with 30 cm of BeO and a gas pressure of 10 atm at 300 K the neutron creation due to the (n, 2n) reaction is 11.7 percent of the total neutron source. The mean free path (mfp) of neutrons in the 30 cm reflector is approximately 1.53 cm for all pressures of uranium-235 gas. Inside the core, for 5 atm of uranium-235 gas the mfp is approximately 804 cm, for 10 atm it is approximately 421 cm, for 15 atm it is approximately 288 cm, and for 20 atm it is approximately 219 cm.

Tungsten-184 Reflector

The use of tungsten-184 makes it very difficult to achieve the prerequisite subcritical state for the fast PMI-GCR model. First, the thickness of a tungsten reflector is examined by plotting the k_{eff} versus reflector thickness for 5, 10, 15, and 20 atm gas at 300 K (Figure 24). It can clearly be seen that the neutron multiplication factor begins to level out at a thickness of approximately 15 cm of tungsten. Figure 25 shows the reactivity versus tungsten thickness, which also shows the values converging on 15 cm.

Next, the desired subcritical state was evaluated (Figure 26) with a tungsten reflector thickness of 15 cm. A uranium-235 gas pressure of about 60 atm at 300 K achieves a subcritical state of about 0.99. When compared to the thermal PMI-GCR model the use of a tungsten reflector causes the system be almost three times heavier. Weight and the extreme operating pressures eliminates the fast PMI-GCR model from being a practical possibility for space applications. The mean neutron lifetime is approximately half a microsecond and increases as pressure decreases or tungsten thickness increases (Figure 27). Analysis of the flux (Figure 28) shows that the almost all of the neutrons never make it to the scatter resonances in tungsten-184 or the fission resonances in uranium-235. The fast PMI-GCR cannot be successfully run with this configuration and therefore should be eliminated as a possible design.

The mean free path (mfp) of neutrons in the 15 cm reflector is approximately 1.94 cm for all pressures of uranium-235 gas. Inside the core, for 60 atm of uranium-235 gas the mfp is approximately 794 cm.

Comparative Analysis of Additional Reflector Materials

Beryllium, with a Z of 4, sits in between carbon (Z=6) and both isotopes of hydrogen (Z=1). Although both graphite and carbon have excellent moderating properties, BeO is still the preferred choice for the PMI-GCR. Zirconium hydride has a saturation thickness of approximately 8 cm for any of the 4 pressures tested (Figure 29) because it has an absorption cross section approximately 40 times higher than BeO. However, the operating pressure for a reactor using this core will be significantly higher than that of 10 atm at 300 K determined for the BeO moderated reactor. Also

contributing is the (n,2n) reaction in beryllium-9, which is like an additional fission source. Twelve percent of the source neutrons generated in the BeO reflected core came from this reaction. This would make it easier to achieve criticality in any core where most of the moderation was done in the beryllium, like the PMI-GCR.

Zirconium deuteride has a saturation thickness almost three times greater than zirconium hydride, about 24 cm, primarily because of deuterium having a neutron in its nucleus (Figure 31). The added mass means that a fission neutron cannot transfer as much of its energy per collision to the deuterium nucleus and therefore requires more collisions. However, when zirconium deuteride is used as a reflector it achieves criticality at lower pressures because deuterium is essentially transparent to neutron absorption. The exact value of the thickness of ZrD_2 is not specifically known since it is difficult to model in MCNP. The error may be large because MCNP does not have a thermal scattering kernel for deuterium in this molecule and therefore treats deuterium as a free gas. When examining the free gas model of $Zr + H_2$ and comparing it to the model that uses the thermal scattering kernel, ZrH_2, there is an error of about 3.5% which is very significant when evaluating k_{eff}. (Figure 30)

Graphite, which is used in some reactor types, is about as high as one can go on the elemental chart and still get adequate neutron thermalization. With six protons and an average of 6 neutrons, a fission neutron must undergo many collisions in order to slow down to thermal energies. Therefore, graphite has a saturation thickness of just over 40 cm (Figure 32). It has a very low absorption cross section, but because of its bulkiness it would not be a desirable material for a PMI-GCR reflector.

Simulated Shockwave

With the pressure and thickness known for the subcritical states of the fast and thermal PMI-GCR models a simulated shockwave analysis can be performed. Keeping the mass in the core constant a 100 atm shockwave interaction was placed at the center of the core, with the remaining uranium-235 gas distributed evenly on either side (see Figure 16 and Table 6). Tables 7 and 8 show the densities and pressures for the thermal and fast reflector models, respectively. The width of the high pressure zone is varied in 5 cm increments. Both of the cores achieve a supercritical state (Figures 33 and 34) which shows that in theory a shockwave driven system with this simple design should work.

Pressure Coefficient of Reactivity

At pressures lower than 100 atm the pressure coefficient of reactivity changes significantly as the pressure in the core increases or decreases. Afterwards, the pressure coefficient of reactivity converges toward a value of about 0.00035 (Figure 35). This allows for quick evaluations for more realistic operating parameters of a PMI-GCR. Throughout this project, pressures have always been referred to as a number “at 300 K”. This is because when operating temperatures for a PMI-GCR are known from future analysis the pressure coefficient of reactivity will allow an engineer to know what will happen when the pressure increases inside the core. If the average temperature for a PMI-GCR is determined to be 2000 K, then using Equation 1 gives an partial pressure for the uranium-235 of approximately 66.7 atm for a BeO reflected core. Then, using the pressure coefficient of reactivity and a fluid dynamics code to determine the transient pressure increase, an idea of the neutron multiplication factor value can be estimated.

Summary of Results

The effect of the reflector material, density, and thickness on a PMI-GCR's neutron multiplication factor and mean neutron lifetime were studied. A subcritical state of about 0.99 was the prerequisite for both the fast and thermal models. Tungsten-184 achieved the desired subcritical state with a thickness of 15 cm and a gas pressure of about 58 atm at 300 K. BeO achieved the desired subcritical with a thickness of 30 cm and a gas pressure of about 10 atm at 300 K. Although the BeO reflector design is twice as thick as the tungsten-184 reflector design, the overall system weighs three times less than the tungsten-184 model. Because of the costs involved in taking anything into space, lower weight will be preferred over any other parameter.

The mean neutron lifetime for a cylindrical core 5 m in length and 181.8 m in diameter with a 30 cm thick BeO reflector and a uranium-235 gas pressure of 10 atm at 300 K is on the order of a few tenths of a millisecond. Twelve percent of the neutrons generated in the BeO model came from the (n,2n) reaction with beryllium-9. These additional neutrons act like an additional neutron source and along with the relatively low absorption cross section allow the core to become critical at lower pressures than any of the other materials studied.

Issues that need to be addressed in the future include coupled aeroacoustic-neutronic models to determine the effects of the shockwave motion inside the core. Detailed information must be gathered, by both computer modeling and experimental analysis, on the effects of a shockwave traveling at supersonic speeds through a fissioning gas.

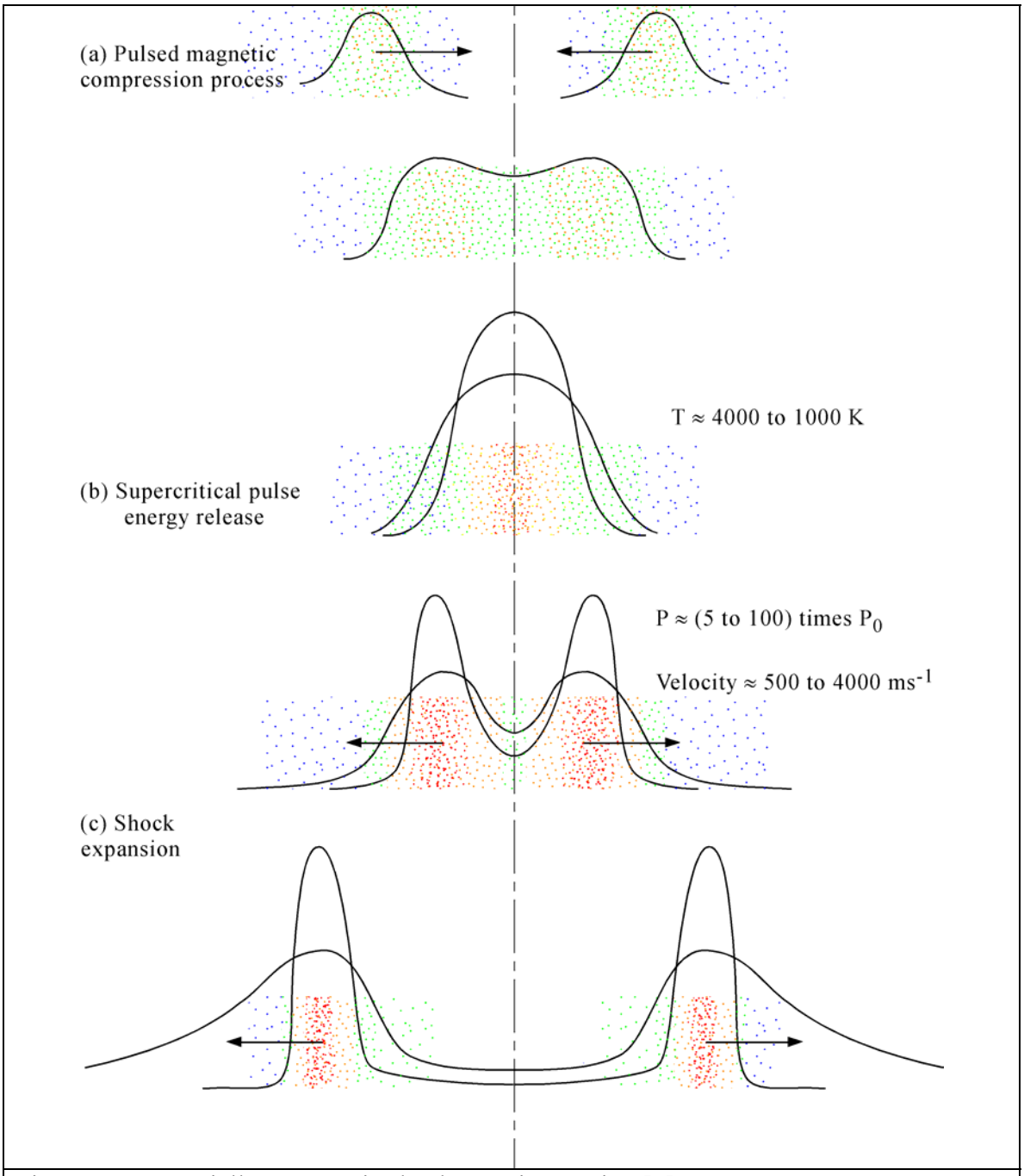

Figure 11. An axially symmetric shockwave interaction.[9]

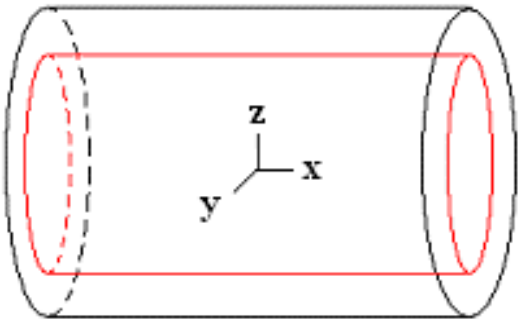

Figure 12. 3-dimensional model of the PMI-GCR. The core, outlined in red, is surrounded laterally by a reflector.

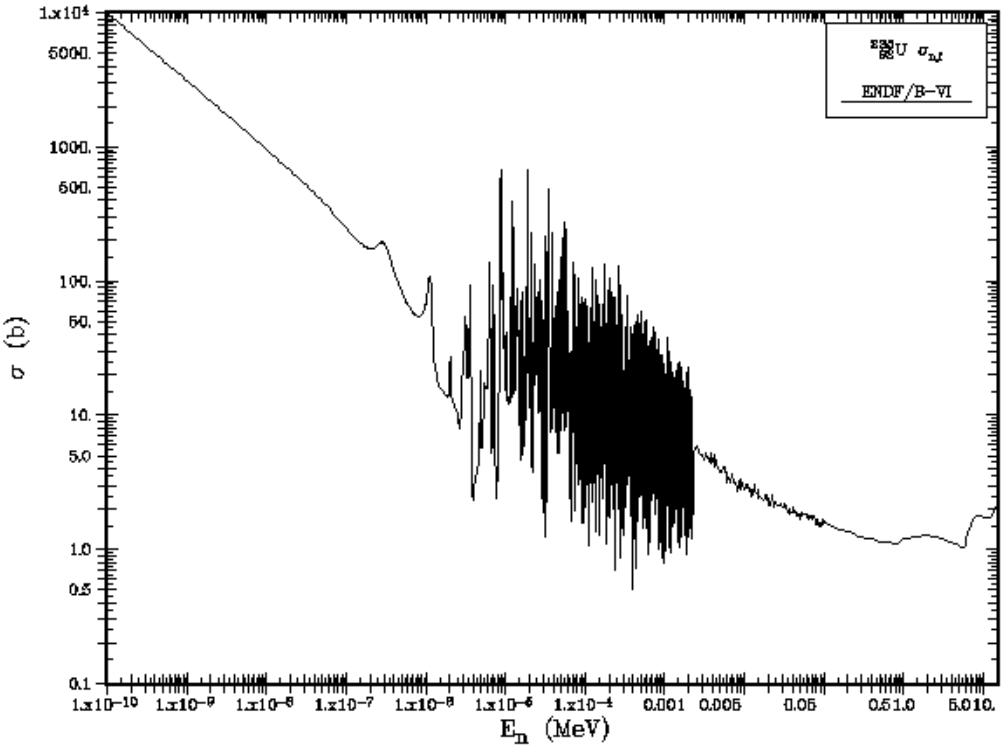

Figure 13. Microscopic fission cross section for uranium-235 at 300 K for 1.00E-10 MeV to 15.0 MeV neutrons.

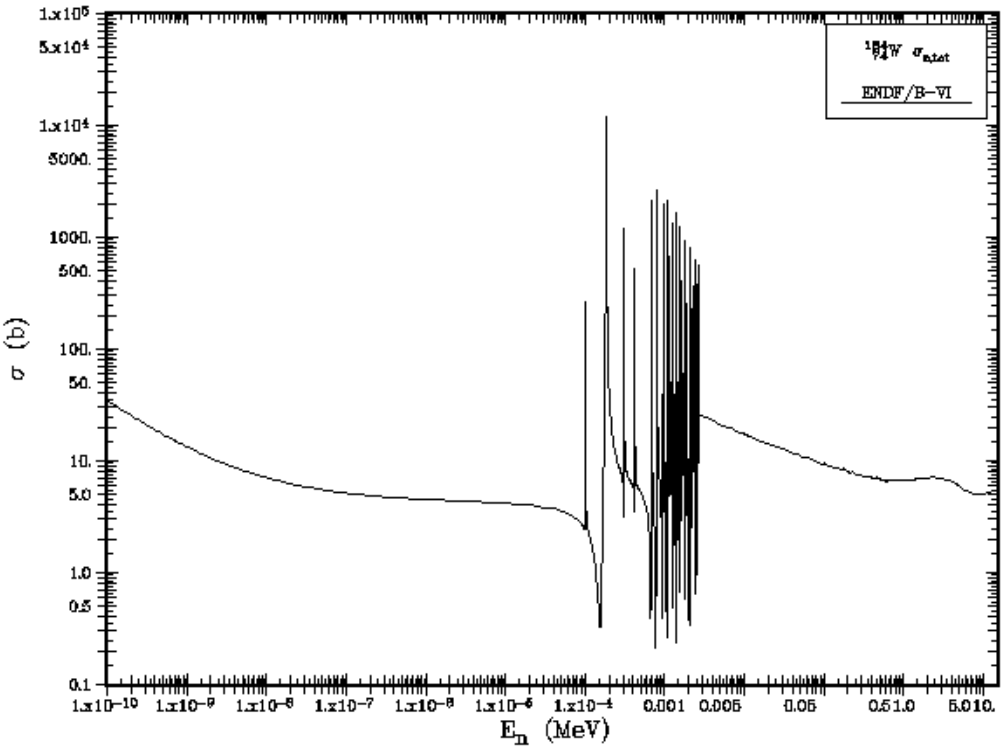

Figure 14. Total microscopic cross section for tungsten-184 at 300 K for 1.00E-10 MeV to 15.0 MeV neutrons.

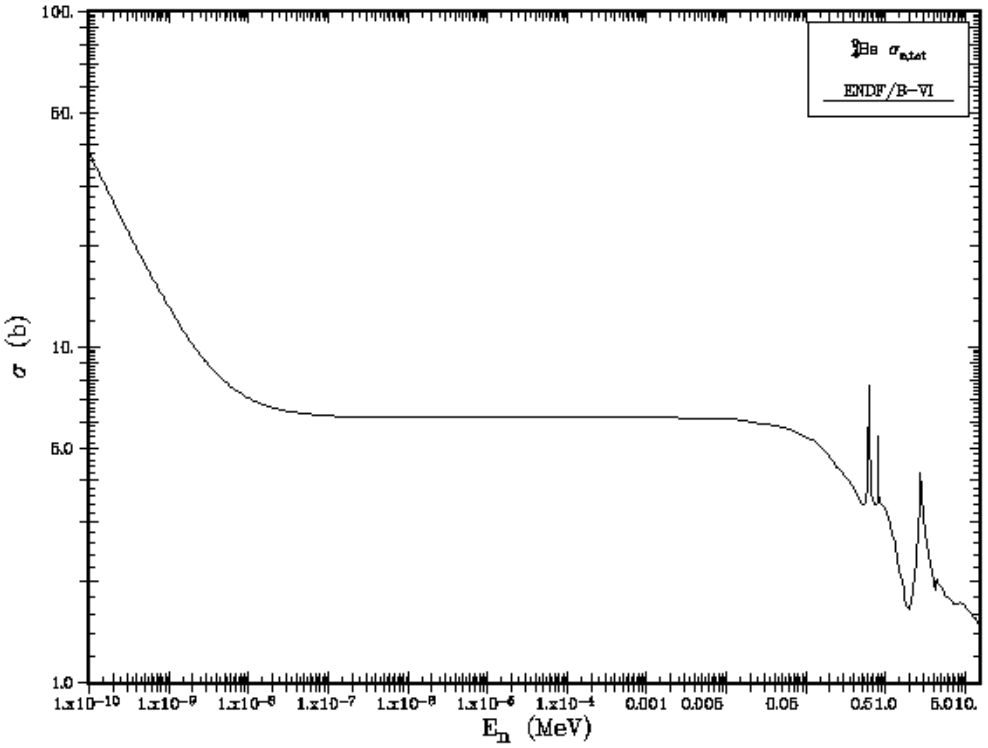

Figure 15. Total microscopic cross section for beryllium-9 at 300 K for 1.00E-10 MeV to 15.0 MeV neutrons.

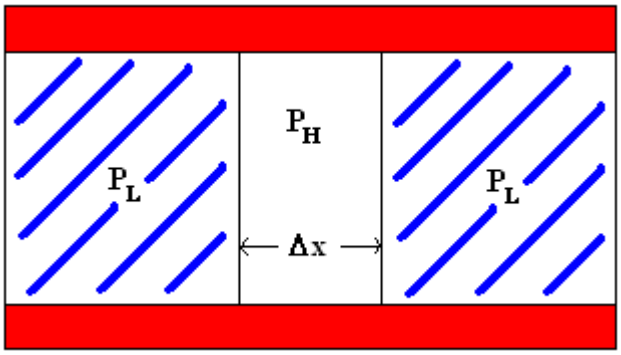

Figure 16. The high pressure region, P_H, has a gas pressure of 100 atm at 300 K and the surrounding regions have a lower pressure, P_L, evenly distributed of the remaining fuel mass of the subcritical core solved for in the previous section.

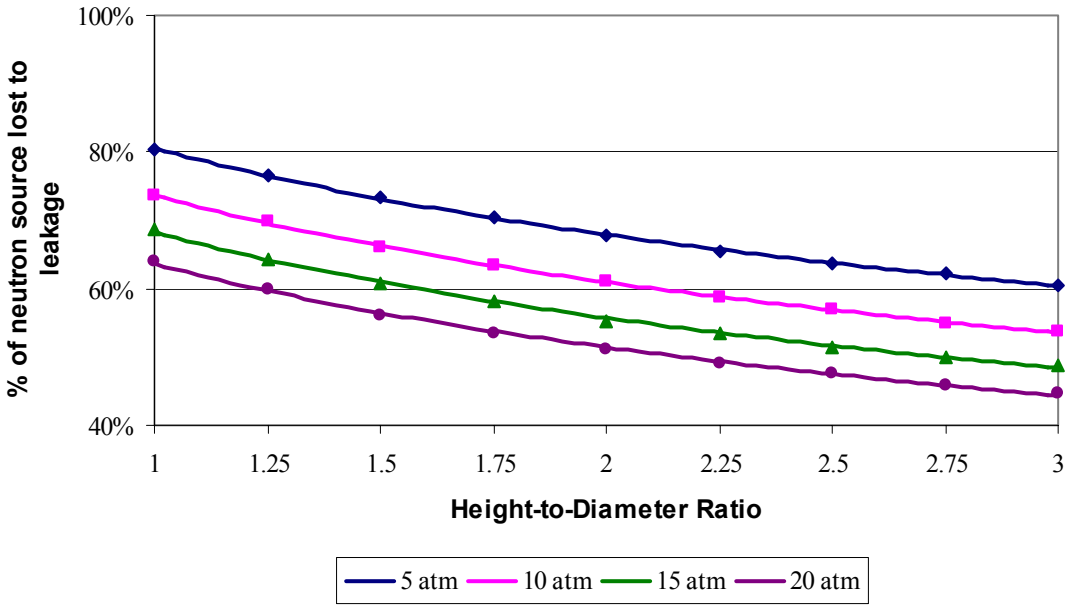

Figure 17. Percent of source neutrons lost to leakage versus the height-to-diameter ratio of the core for 5, 10, 15, and 20 atm gas at 300 K for a constant volume reactor of 30 m^3. The average uncertainty for the evaluated leakage is half a percent.

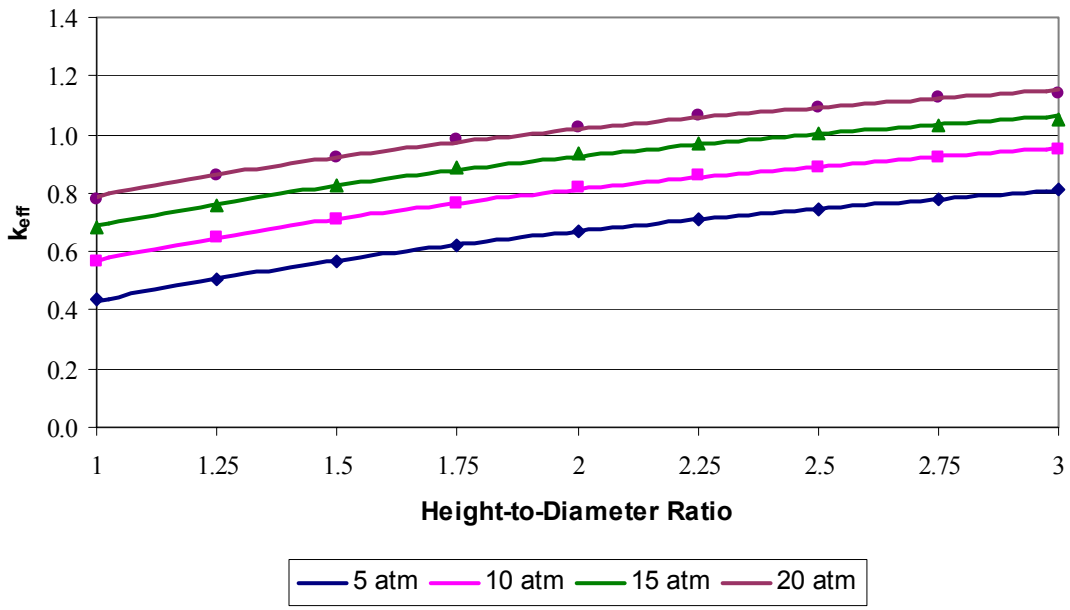

Figure 18. Neutron multiplication factor versus the height-to-diameter ratio of the core for 5, 10, 15, and 20 atm gas at 300 K. The average uncertainty is approximately ± 0.0018.

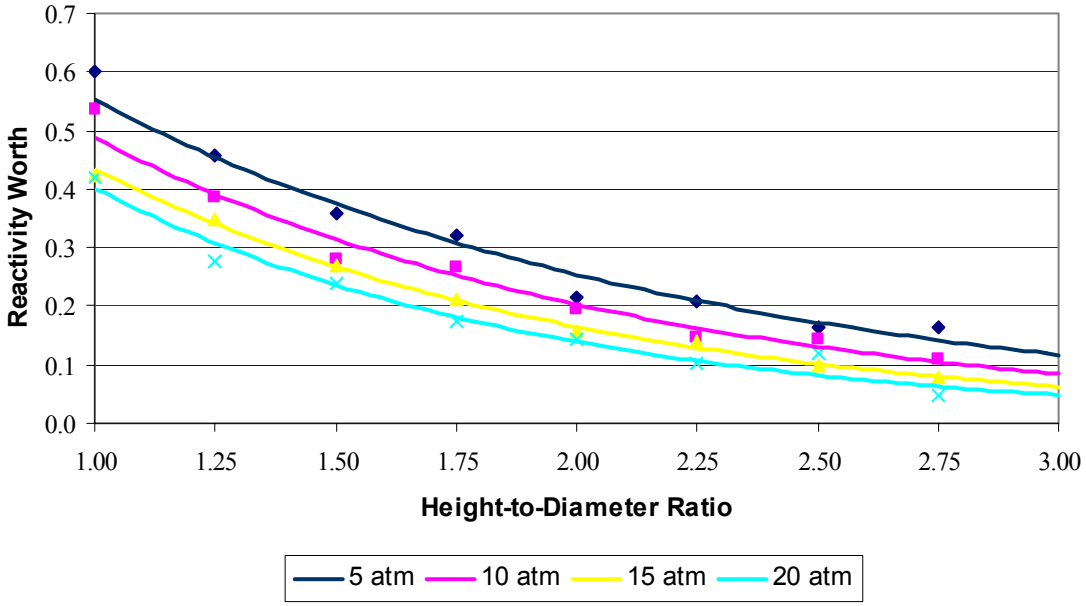

Figure 19. Reactivity worth (Δk/k per height-to-diameter ratio step) versus the height-to-diameter ratio of the core for 5, 10, 15, and 20 atm gas at 300 K.

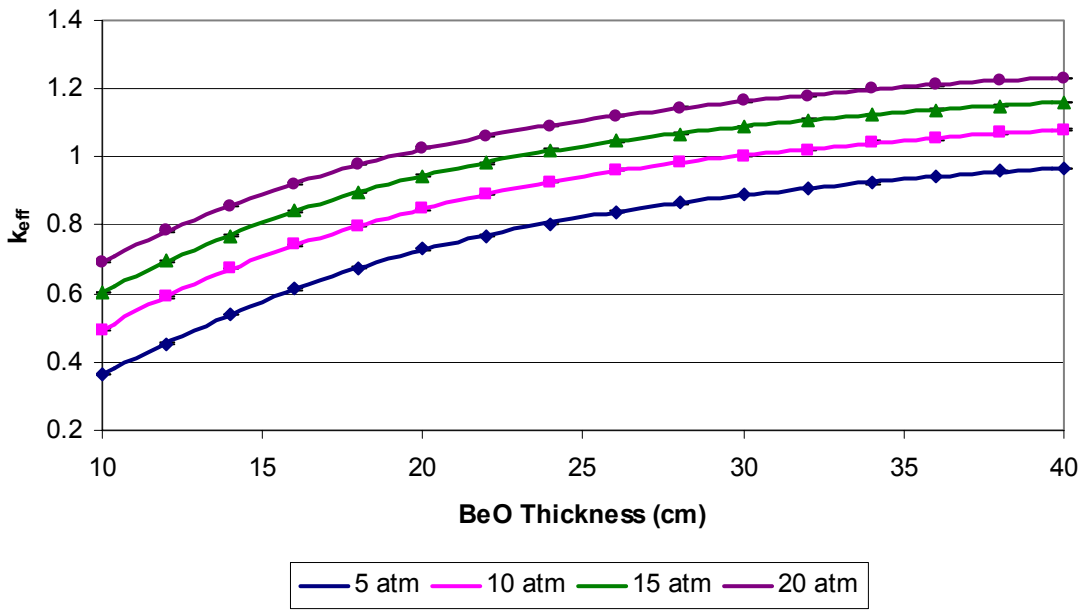

Figure 20. k_{eff} versus BeO thickness for 5, 10, 15, and 20 atm uranium-235 gas at 300 K. The average standard deviation is ±0.0020.

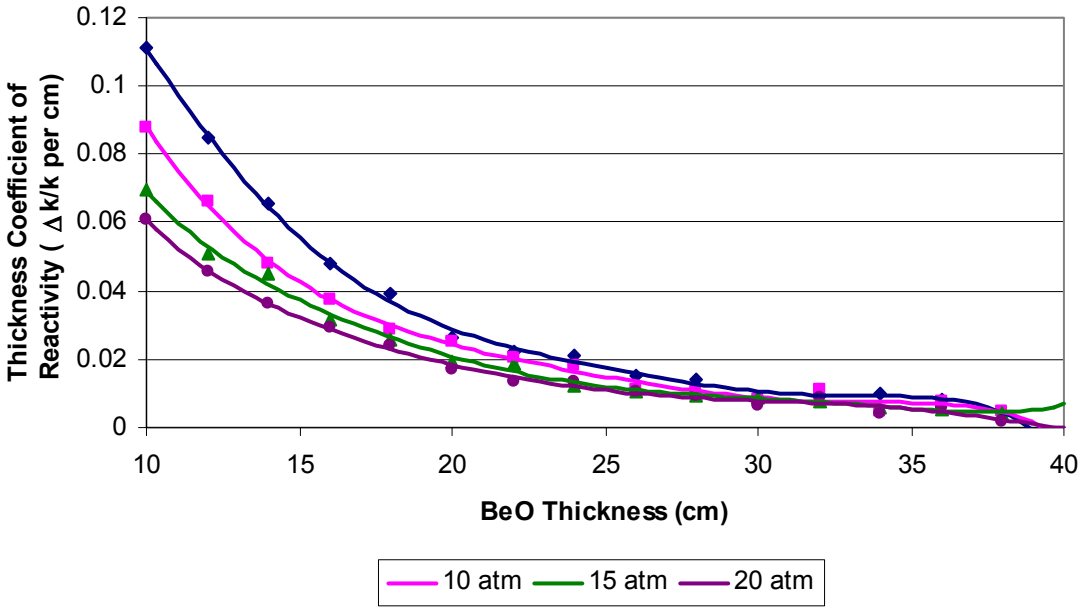

Figure 21. Thickness coefficient of reactivity (Δk/k per cm) versus BeO thickness for 5, 10, 15, and 20 atm gas at 300 K.

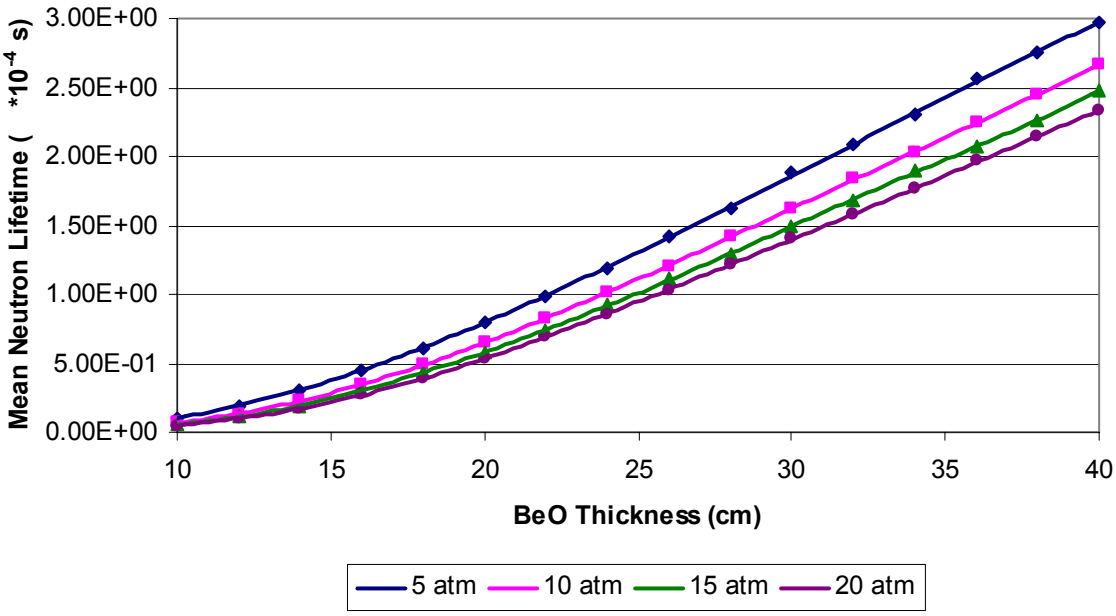

Figure 22. Mean neutron lifetime (10^{-4} s) versus BeO thickness for 5, 10, 15, and 20 atm gas at 300 K.

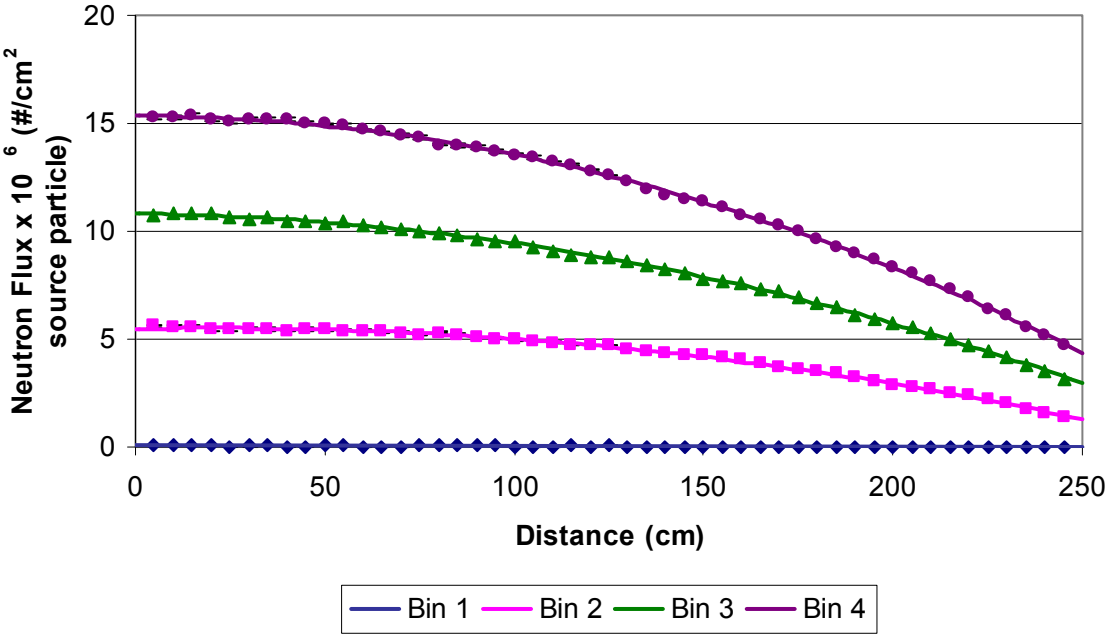

Figure 23. 4 bin axial flux, in neutrons per cm^2, versus distance from the center of the core in cm. Bin 1 covers the energy range from 1.0E-10 MeV to 1.0E-07 MeV and has an average deviation of 9.8 %. Bin 2 covers the energy range from 1.0E-07 MeV to 1.0E-02 MeV and has an average deviation of 1.4 %. Bin 3 covers the energy range from 1.0E-02 MeV to 0.4 MeV and has an average deviation of 1.0%. Bin 4 covers the energy range from 0.4 MeV to 15.0 MeV and has an average deviation of 0.8%.

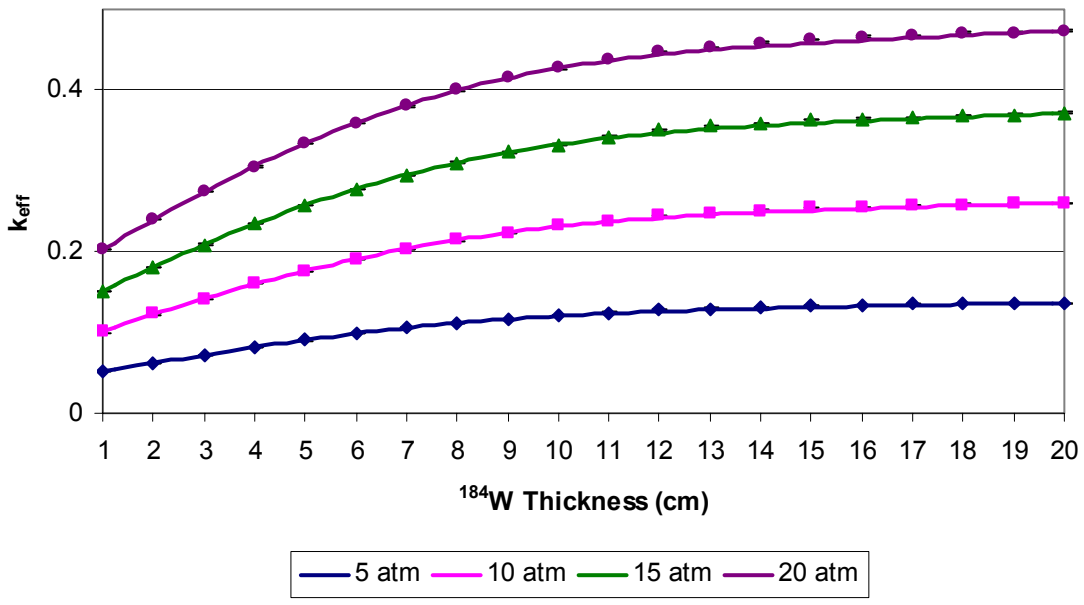

Figure 24. k_{eff} versus tungsten thickness for 5, 10, 15, and 20 atm gas at 300 K. The average standard deviation is ± 0.0005.

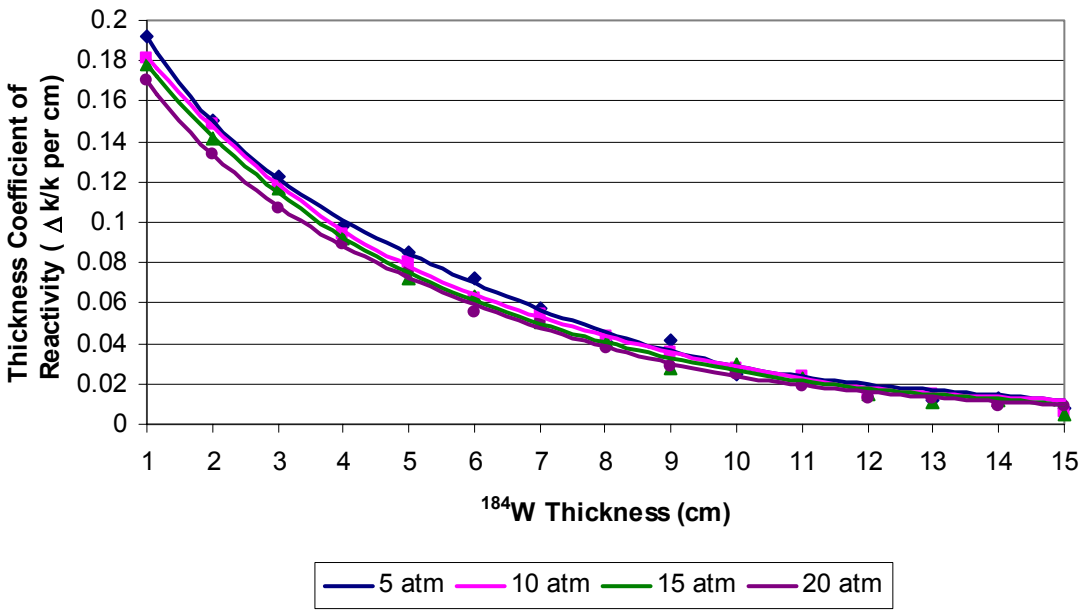

Figure 25. Thickness coefficient of reactivity (Δk/k per cm) versus tungsten thickness for 5, 10, 15, and 20 atm gas at 300 K.

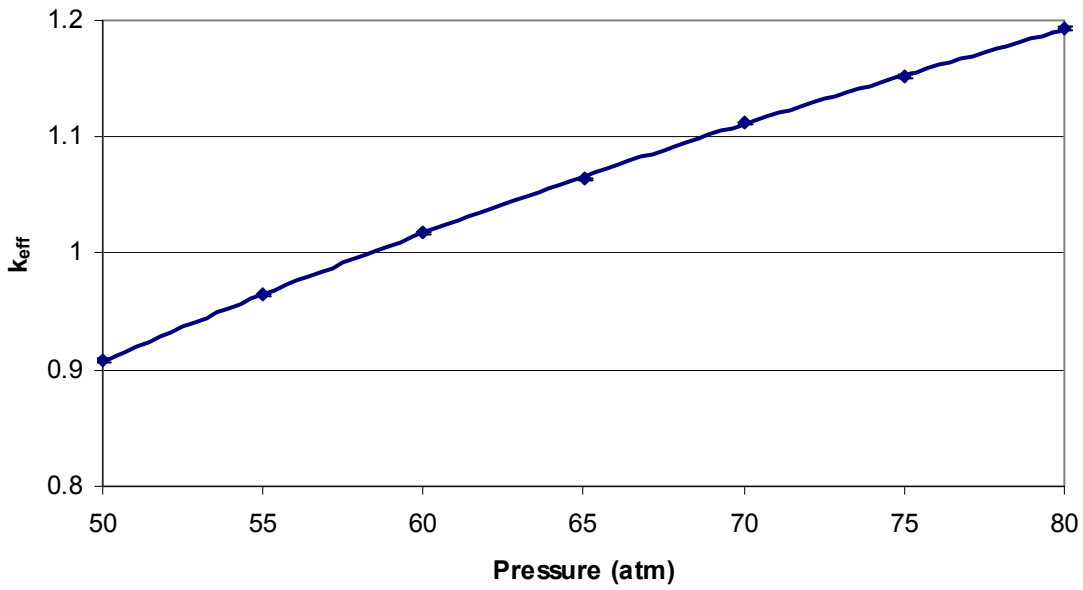

Figure 26. keff versus uranium 235 pressure from 50 to 80 atm at 300 K with a tungsten reflector thickness of 15 cm. The average standard deviation is ± 0.0013.

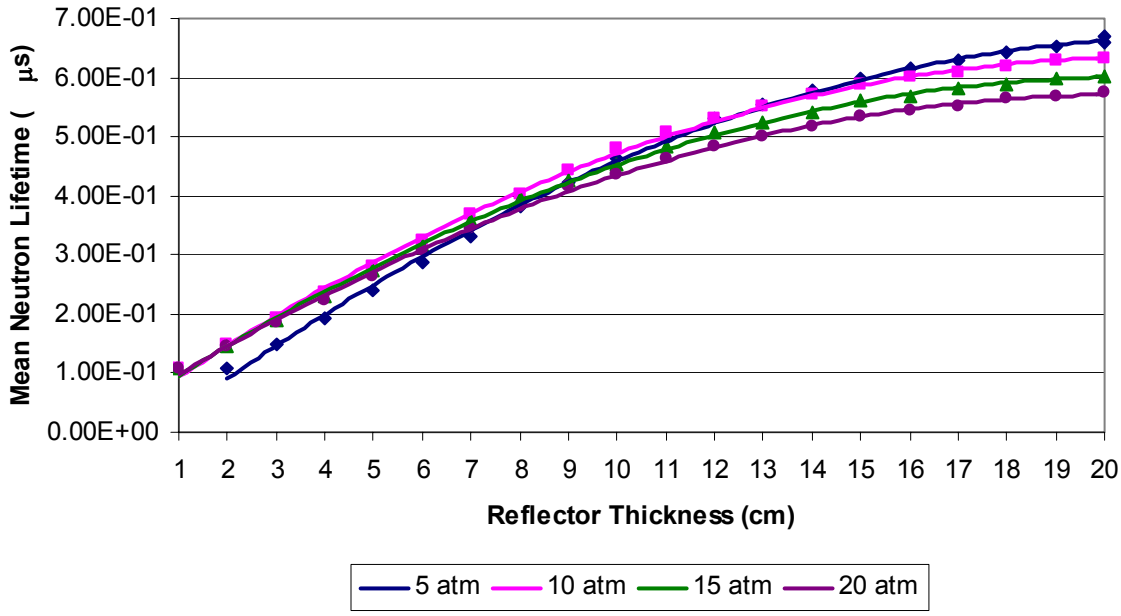

Figure 27. Average time (µs) to particle termination versus tungsten thickness for 5, 10, 15, and 20 atm gas.

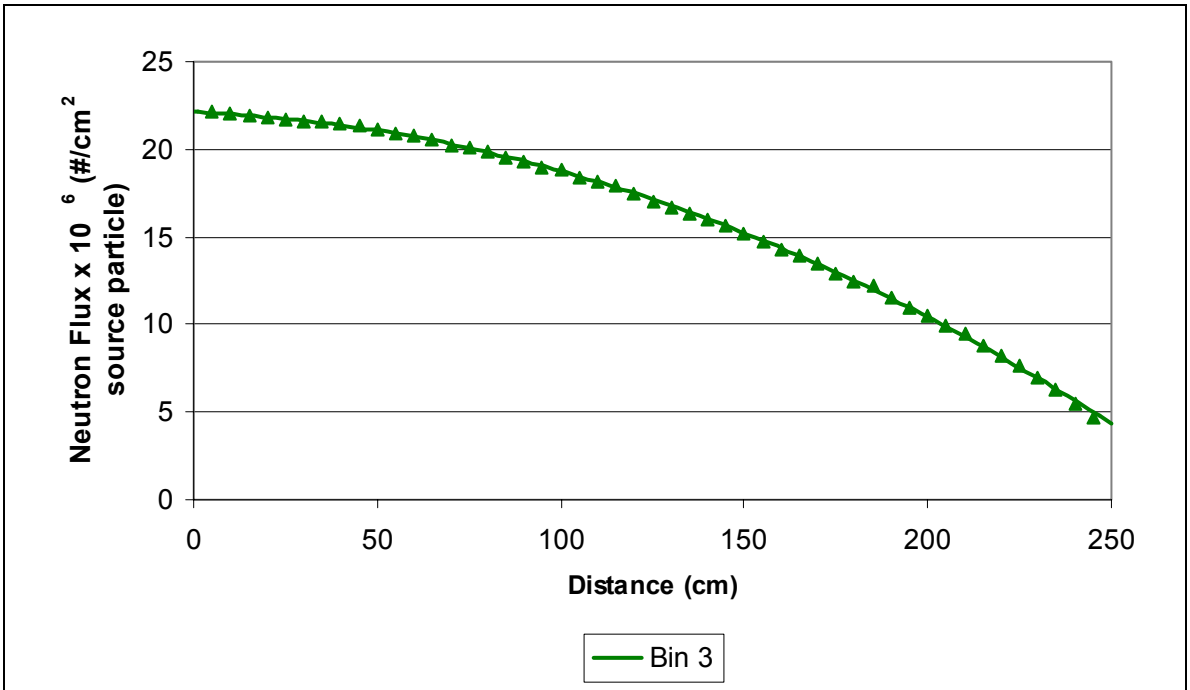

Figure 28. Out of the 3 bins used to analyze the neutron flux for a core with a 15 cm tungsten reflector at 60 atm at 300 K only one bin contained a significant percentage of source neutrons. This is unfortunate because most of the neutrons make it to neither the scatter resonances of tungsten-184, nor the fission resonances of uranium-235. Therefore tungsten-184 is not an appropriate material for a fast PMI-GCR reactor. Bin 3 has an average standard deviation of 0.6 %.

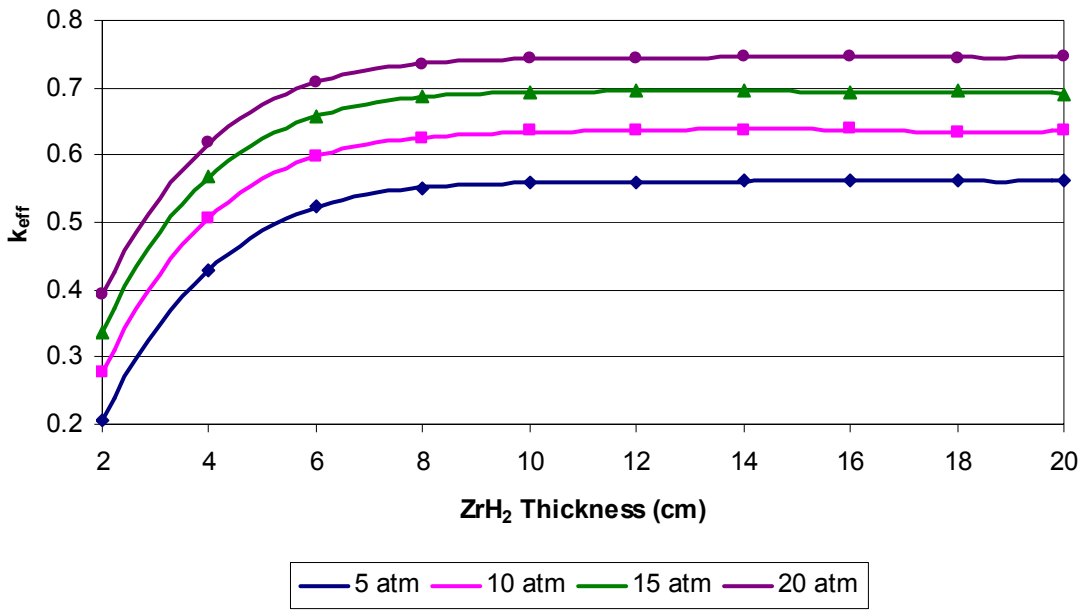

Figure 29. k_{eff} versus ZrH_2 thickness for 5, 10, 15, and 20 atm uranium-235 gas at 300 K. The average standard deviation is ± 0.0017.

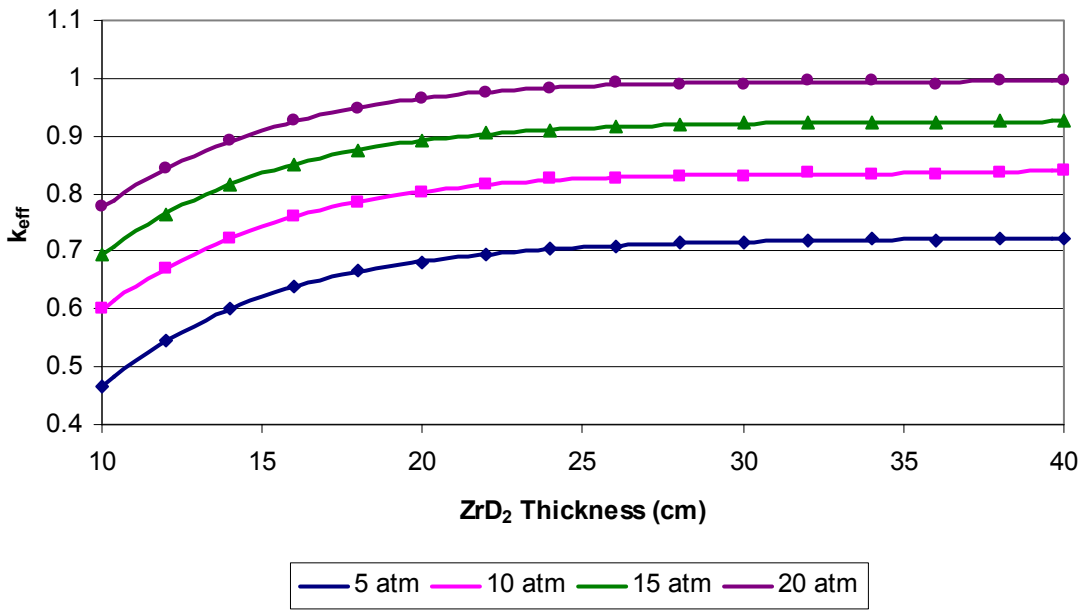

Figure 30. k_{eff} versus ZrD_2 thickness for 5, 10, 15, and 20 atm uranium-235 gas at 300 K. The average standard deviation is ± 0.00218.

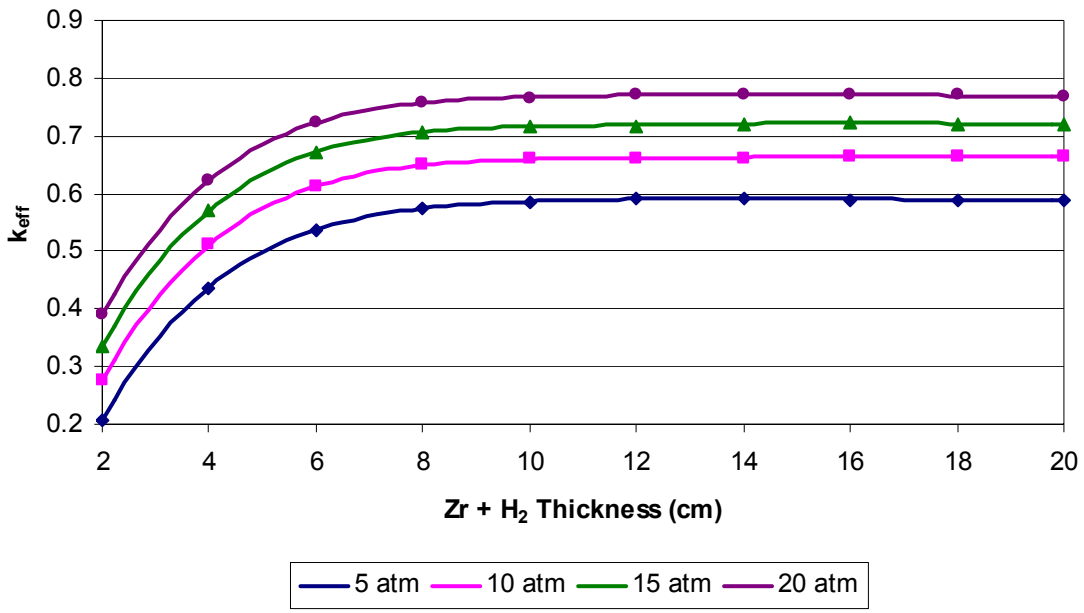

Figure 31. k_{eff} versus Zr + H_2 thickness for 5, 10, 15, and 20 atm uranium-235 gas at 300 K. The average standard deviation is ± 0.0017.

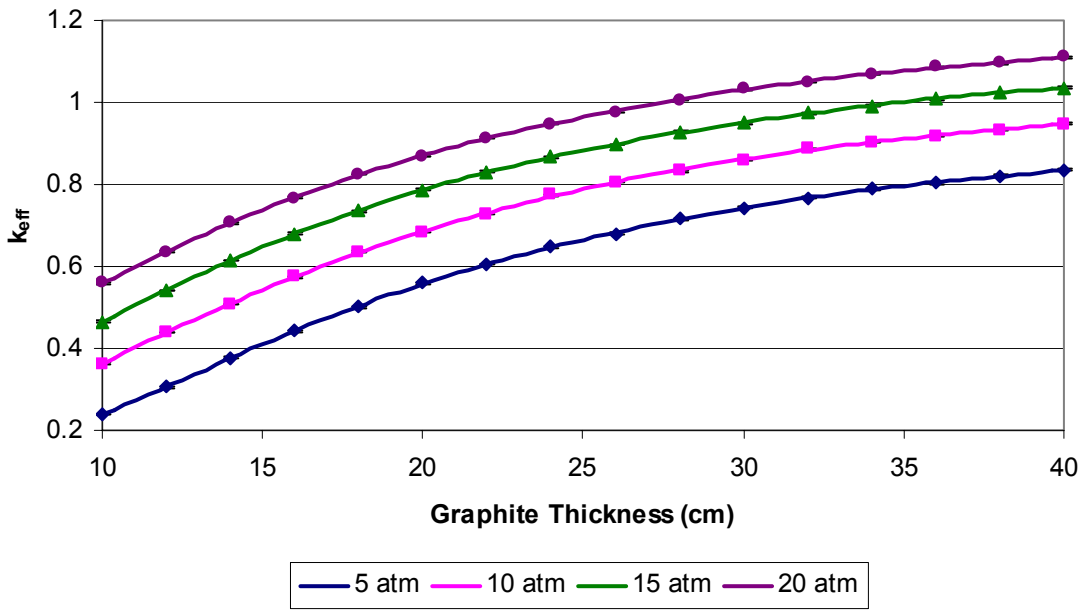

Figure 32. k_{eff} versus high density graphite thickness for 5, 10, 15, and 20 atm uranium-235 gas at 300 K. The average standard deviation is ± 0.0019.

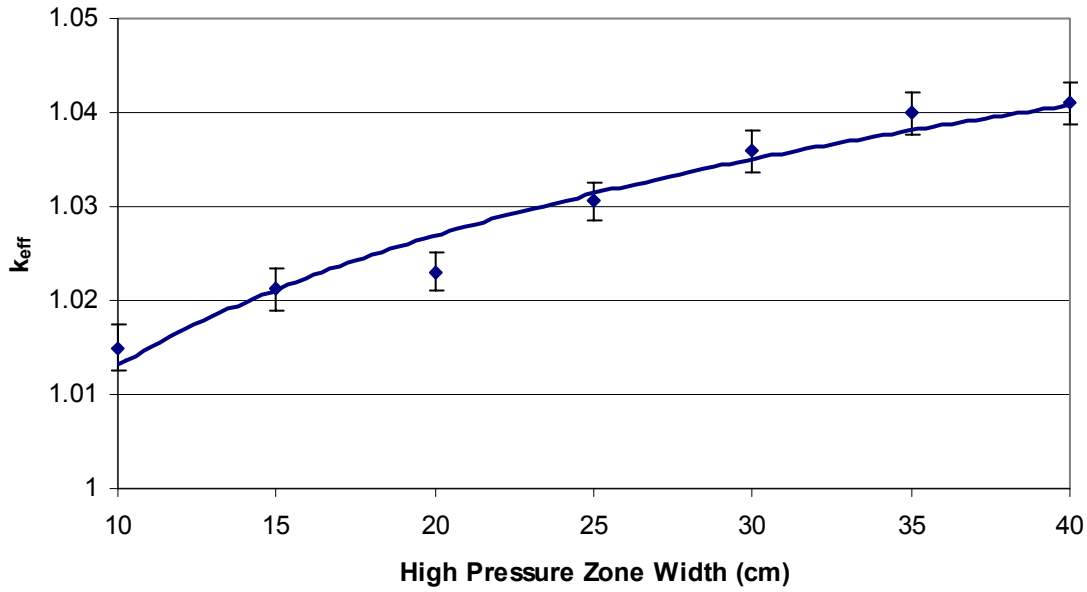

Figure 33. k_{eff} versus high pressure zone width for a 30 cm BeO moderated core at 300 K.

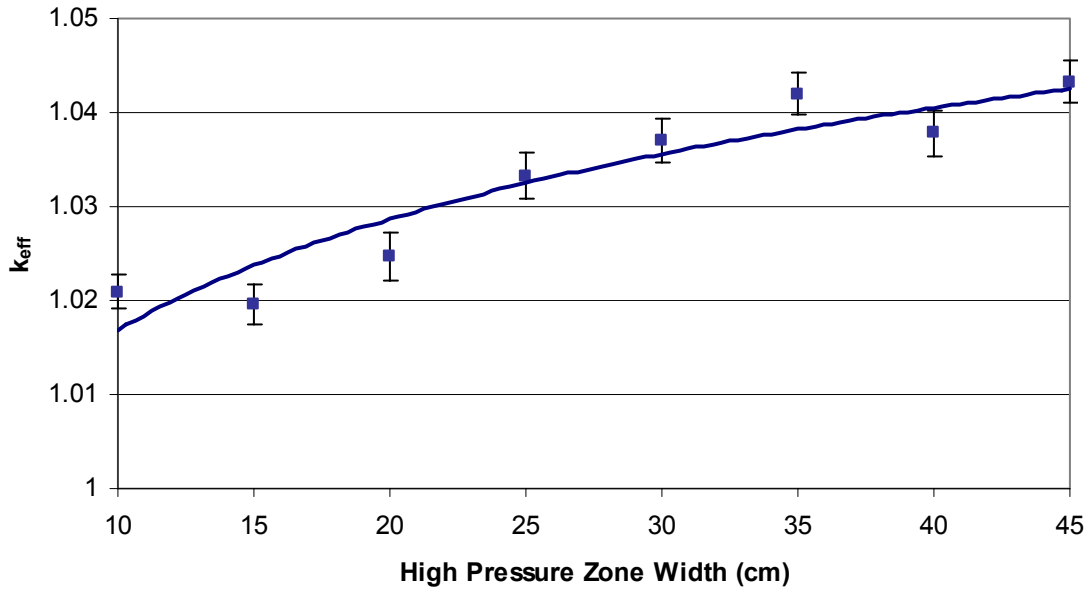

Figure 34. k_{eff} versus high pressure zone width for a 15 cm tungsten reflected core at 300 K.

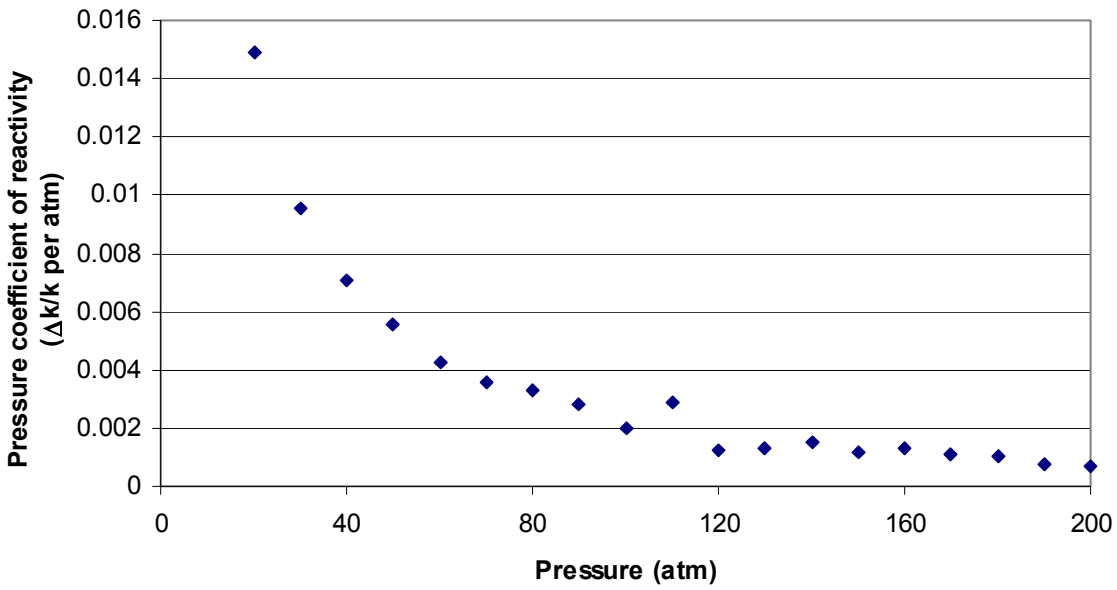

Figure 35. Pressure coefficient of reactivity (Δk/k per atm) for a 30 cm BeO moderated core. The level of uncertainty calculated by MCNP for the k_{eff}, on average approximately half a percent, may be too high for this calculation. This would cause artifacts like the point at 100 atm to stand out away from the norm.

REFERENCES

[1]. Diaz, Nils J., Preface: Gaseous Core Reactors; Nuclear Technology, Vol. 69, May 1985.
[2]. K. Thom, R. T. Schneider, and F. C. Schwenk, "Physics and Potentials of Fissioning Plasmas for Space Power Propulsion," 25th Congress of the International Astronautical Federation, Amsterdam, 30 September to 5 October 1974.
[3]. N. Diaz, S. Anghaie, E. T. Dugan, and I. Maya, "Gas Core Reactor Concepts and Technology," AIAA 91-3582, AIAA/NASA/OAI Conference on Advanced SEI Technologies, Cleveland, OH, September, 1991.
[4]. I. Maya, S. Anghaie, N. J. Diaz, and E. T. Dugan, "Ultra Temperature Vapor Core Reactor-MHD System for Space Nuclear Electric Power," AIAA 91-3632, AIAA/NASA/OAI Conference on Advanced SEI Technologies, September 4-6, 1991, Cleveland, OH.
[5]. N. J. Diaz, S. Anghaie, E. T. Dugan, and I. Maya, "Ultrahigh Temperature vapor Reactor and Magneto Conversion for Multi-Megawatt Space Power Generation," Space Power, Vol. 8, Nos. 1 / 2, 1989.
[6]. S. Anghaie, "Uranium Droplet Core Nuclear Rocket," AIAA/NASA/OAI Conference on Advanced SEI Technologies, Cleveland, OH, September, 1991.
[7]. Begg, L. L. and Engdahl, E. H., Advanced Radiator Concepts, *Proceedings of the 24th Intersociety Energy Conversion Engineering Conference*, 1989
[8]. Dugan, Edward T., The Nuclear Piston Engine and Pulsed Gaseous Core Reactor Power Systems. PhD Thesis, University of Florida, 1976.
[9]. INSPI Internal Report, 1992, University of Florida
[10]. Lamarsh, John R., Introduction to Nuclear Engineering, Second Edition; Addison-Wesley Publishing (1983)